REFERENCES

Aljohani, A., & Alharbe, N. (2022). Generating Synthetic Images for Healthcare with Novel Deep Pix2pix GAN. Electronics, 11(21), 3470.

Bilal, A., Sun, G., & Mazhar, S. (2021). Finger-Vein Recognition using a Novel Enhancement Method with Convolutional Neural Network. Journal of the Chinese Institute of Engineers, 44(5), 407-417.

Boucetta, A., & Boussaad, L. (2022). Biometric Authentication using Finger-Vein Patterns with Deep-Learning and Discriminant Correlation Analysis. International Journal of Image and Graphics, 22(01), 2250013.

Chang, J., Lai, T., Yang, L., Fang, C., Li, Z., & Fujita, H. (2023). FV-DGNN: A Distance-Based Graph Neural Network for Finger Vein Recognition. IEEE Transactions on Instrumentation and Measurement.

Chawla, B., Tyagi, S., Jain, R., Talegaonkar, A., & Srivastava, S. (2021). Finger Vein Recognition using Deep Learning. In Proceedings of International Conference on Artificial Intelligence and Applications: ICAIA 2020 (pp. 69-78). Springer Singapore.

Chen, C., Wu, Z., Zhang, J., Li, P., & Azmat, F. (2017). A Finger Vein Recognition Algorithm based on Deep Learning. International Journal of Embedded Systems, 9(3), 220-228.

Dahea, W., & Fadewar, H. S. (2020, October). Finger Vein Recognition System based on Multi-Algorithm of Fusion of Gabor Filter and Local Binary Pattern. In 2020 Fourth International Conference on I-SMAC (IoT in Social, Mobile, Analytics and Cloud) (I-SMAC) (pp. 403-410). IEEE.

Devkota, N., & Kim, B. W. (2024). Finger Vein Recognition using Densenet with a Channel Attention Mechanism and Hybrid Pooling. Electronics, 13(3), 501.

Fang, Y., Wu, Q., & Kang, W. (2018). A Novel Finger Vein Verification System based on Two-Stream Convolutional Network Learning. Neurocomputing, 290, 100-107.

Fanjiang, Y. Y., Lee, C. C., Du, Y. T., & Horng, S. J. (2021). Palm Vein Recognition based on Convolutional Neural Network. Informatica, 32(4), 687-708.

Goodfellow, I., Pouget-Abadie, J., Mirza, M., Xu, B., Warde-Farley, D., Ozair, S., & Bengio, Y. (2014). Generative Adversarial Nets. Advances in Neural Information Processing Systems, 27.

Gumusbas, D., Yildirim, T., Kocakulak, M., & Acir, N. (2019). Capsule network for finger-vein-based biometric identification. In 2019 IEEE Symposium Series on Computational Intelligence (SSCI) (pp. 437-441). IEEE.

Hao, Z., Fang, P., & Yang, H. (2020). Finger Vein Recognition based on Multi-Task Learning. In Proceedings of the 2020 5th International Conference on Mathematics and Artificial Intelligence (pp. 133-140).

Hijazi, S., Kumar, R., & Rowen, C. (2015). Using Convolutional Neural Networks for Image Recognition. Cadence Design Systems Inc.: San Jose, CA, USA, 9(1).

Hong, H. G., Lee, M. B., & Park, K. R. (2017). Convolutional Neural Network based Finger-Vein Recognition using NIR Image Sensors. Sensors, 17(6), 1297.

Hou B., Zhang, H., & Yan, R. (2022). Finger-Vein Biometric Recognition: A Review. IEEE Transactions on Instrumentation and Measurement, 71, 1-26.

Hou, B., & Yan, R. (2019). Convolutional Autoencoder Model for Finger-Vein Verification. IEEE Transactions on Instrumentation and Measurement, 69(5), 2067-2074.

Huang, B., Dai, Y., Li, R., Tang, D., & Li, W. (2010). Finger-Vein Authentication based on Wide Line Detector and Pattern Normalization. In 2010 20th International Conference on Pattern Recognition (pp. 1269-1272). IEEE.

Huang, H., Lin, L., Tong, R., Hu, H., Zhang, Q., Iwamoto, Y., & Wu, J. (2020). UNET 3+: A Full-Scale Connected UNET for Medical Image Segmentation. In ICASSP 2020-2020 IEEE International Conference on Acoustics, Speech and Signal Processing (ICASSP) (pp. 1055-1059). IEEE.

Huang, H., Liu, S., Zheng, H., Ni, L., Zhang, Y., & Li, W. (2017). DeepVein: Novel Finger Vein Verification Methods Based on Deep Convolutional Neural Networks. In 2017 IEEE International Conference on Identity, Security and Behaviour Analysis (ISBA) (pp. 1-8). IEEE.

Huang, Z., & Guo, C. (2021). Robust Finger Vein Recognition based on Deep CNN with Spatial Attention and Bias Field Correction. International Journal on Artificial Intelligence Tools, 30(01), 2140005.

Ismail, B., & Mohamed, O. Z. (2019). Finger Vein Image Enhancement Technique Based on Gabor Filter and Discrete Cosine Transform. Journal of Telecommunication, Electronic and Computer Engineering (JTEC), 11(2), 43-48.

Jalilian, E., & Uhl, A. (2018). Finger-Vein Recognition using Deep Fully Convolutional Neural Semantic Segmentation Networks: The Impact of Training Data. In 2018 IEEE International Workshop on Information Forensics and Security (WIFS) (pp. 1-8). IEEE.

Jalilian, E., & Uhl, A. (2019). Enhanced Segmentation-CNN based Finger-Vein Recognition by Joint Training with Automatically Generated and Manual Labels. In 2019 IEEE 5th International Conference on Identity, Security, and Behaviour Analysis (ISBA) (pp. 1-8). IEEE.

Kapoor, K., Rani, S., Kumar, M., Chopra, V., & Brar, G. S. (2021). Hybrid Local Phase Quantization and Grey Wolf Optimization based SVM for Finger Vein Recognition. Multimedia Tools and Applications, 80(10), 15233-15271.

Kauba, C., Piciucco, E., Maiorana, E., Campisi, P., & Uhl, A. (2016). Advanced Variants of Feature Level Fusion for Finger Vein Recognition. In 2016 International Conference of the Biometrics Special Interest Group (BIOSIG) (pp. 1-7). IEEE.

Khellat-Kihel, S., Cardoso, N., Monteiro, J., & Benyettou, M. (2014). Finger Vein Recognition using Gabor Filter and Support Vector Machine. In International Image Processing, Applications and Systems Conference (pp. 1-6). IEEE.

Khusnuliawati, H., Fatichah, C., & Soelaiman, R. (2017). Multi-Feature Fusion using SIFT and LEBP for Finger Vein Recognition. TELKOMNIKA (Telecommunication Computing Electronics and Control), 15(1), 478-485.

Kim, J., Kong, H. J., Park, S., Noh, S., Lee, S. R., Kim, T., & Kim, H. C. (2009). Non-Contact Finger Vein Acquisition System using NIR Laser. In Sensors, Cameras, And Systems for Industrial/Scientific Applications X (Vol. 7249, pp. 249-256). SPIE.

Kim, W., Song, J. M., & Park, K. R. (2018). Multimodal Biometric Recognition based on Convolutional Neural Network by The Fusion of Finger-Vein and Finger Shape using Near-Infrared (NIR) Camera Sensor. Sensors, 18(7), 2296.

Kono, M. (2000). A new Method for the Identification of Individuals by using Vein Pattern Matching of a Finger. In Proc. Fifth Symposium on Pattern Measurement, Yamaguchi, Japan, 2000 (pp. 9-12).

Krishnan, A., & Thomas, T. (2023). Finger Vein Recognition based on Anatomical Features of Vein Patterns. IEEE Access, 11, 39373-39384.

Krishnan, H., & Khare, S. (2022). Finger Vein Recognition using Deep Learning. Mathematical Statistician and Engineering Applications, 71(3s), 352-360.

Kuzu, R. S., Piciucco, E., Maiorana, E., & Campisi, P. (2020). On-the-Fly Finger-Vein-based Biometric Recognition using Deep Neural Networks. IEEE Transactions on Information Forensics and Security, 15, 2641-2654.

Lee, E. C., Lee, H. C., & Park, K. R. (2009). Finger Vein Recognition using Minutia-based Alignment and Local Binary Pattern-Based Feature Extraction. International Journal of Imaging Systems and Technology, 19(3), 179-186.

Li, J., Yang, L., Ye, M., Su, Y., & Liu, J. (2022). Finger Vein Verification on different Datasets based on Deep Learning with Triplet Loss. Computational and Mathematical Methods in Medicine, 2022(1), 4868435.

Li, S., Ma, R., Fei, L., & Zhang, B. (2022). Learning Compact Multi Representation Feature Descriptor for Finger-Vein Recognition. IEEE Transactions on Information Forensics and Security, 17, 1946-1958.

Li, Y., Lu, H., Wang, Y., Gao, R., & Zhao, C. (2022). VIT-CAP: A Novel Vision Transformer-Based Capsule Network Model for Finger Vein Recognition. Applied Sciences, 12(20), 10364.

Liu, B. C., Xie, S. J., & Park, D. S. (2016). Finger Vein Recognition using Optimal Partitioning Uniform Rotation Invariant LBP Descriptor. Journal of Electrical and Computer Engineering, 2016(1), 7965936.

Liu, F., Yang, G., Yin, Y., & Wang, S. (2014). Singular Value Decomposition based Minutiae Matching Method for Finger Vein Recognition. Neurocomputing, 145, 75-89.

Liu, L., Zhang, D., & You, J. (2007). Detecting Wide Lines using Isotropic Nonlinear Filtering. IEEE Transactions on image processing, 16(6), 1584-1595.

Liu, W., Lu, H., Wang, Y., Li, Y., Qu, Z., & Li, Y. (2023). MMRAN: A Novel Model for Finger Vein Recognition based on a Residual Attention Mechanism, Applied Intelligence, 53(3), 3273-3290.

Liu, Z., & Song, S. (2012). An Embedded Real-Time Finger-Vein Recognition System for Mobile Devices. IEEE Transactions on consumer Electronics, 58(2), 522-527.

Liu, Z., Yin, Y., Wang, H., Song, S., & Li, Q. (2010). Finger Vein Recognition with Manifold Learning. Journal of Network and Computer Applications, 33(3), 275-282.

Lu Yu., Xie, S., & Wu, S. (2019). Exploring Competitive Features using Deep Convolutional Neural Network for Finger Vein Recognition. IEEE access, 7, 35113-35123.

Lu, Y., Yoon, S., Xie, S. J., Yang, J., Wang, Z., & Park, D. S. (2014). Finger Vein Recognition using Generalized Local Line Binary Pattern. KSII Transactions on Internet and Information Systems (TIIS), 8(5), 1766-1784.

Lv, G. L., Shen, L., Yao, Y. D., Wang, H. X., & Zhao, G. D. (2020). Feature-Level Fusion of Finger Vein and Fingerprint Based on a Single Finger Image: The use of Incompletely Closed Near-Infrared Equipment. Symmetry, 12(5), 709.

Ma, B., Wang, K., & Hu, Y. (2023). Finger Vein Recognition Based on Bilinear Fusion of Multiscale Features. Scientific Reports, 13(1), 249.

Ma, H., Hu, N., & Fang, C. (2021). The Biometric Recognition System based on Near-Infrared Finger Vein Image. Infrared Physics & Technology, 116, 103734.

Ma, X., & Luo, X. (2023). Finger Vein Recognition Method based on Ant Colony Optimization and Improved EfficientNetV2. Math Biosci Eng, 20(6), 11081-11100.

Madhusudhan, M. V., Udaya Rani, V., & Hegde, C. (2023). Finger Vein Recognition Model for Biometric Authentication using Intelligent Deep Learning. International Journal of Image and Graphics, 23(03), 2240004.

Meng, G., Fang, P., & Zhang, B. (2017). Finger Vein Recognition based on Convolutional Neural Network. In MATEC Web of Conferences (Vol. 128, p. 04015). EDP Sciences.

Meng, X., Yang, G., Yin, Y., & Xiao, R. (2012). Finger Vein Recognition based on Local Directional Code. Sensors, 12(11), 14937-14952.

Miura, N., Nagasaka, A., & Miyatake, T. (2004). Feature Extraction of Finger-Vein Patterns Based on Repeated Line Tracking and its Application to Personal Identification. Machine vision and applications, 15, 194-203.

Miura, N., Nagasaka, A., & Miyatake, T. (2007). Extraction of Finger-Vein Patterns using Maximum Curvature Points in Image Profiles. IEICE TRANSACTIONS on Information and Systems, 90(8), 1185-1194.

Mohsin, A. H., Zaidan, A. A., Zaidan, B. B., Albahri, O. S., Ariffin, S. A. B., Alemran, A., & Garfan, S. (2020). Finger Vein Biometrics: Taxonomy Analysis, Open Challenges, Future Directions, and Recommended Solution for Decentralised Network Architectures. IEEE Access, 8, 9821-9845.

Nagaraju, M., Chawla, P., & Kumar, N. (2022). Performance Improvement of Deep Learning Models using Image Augmentation Techniques. Multimedia Tools and Applications, 81(7), 9177-9200.

Noh, K. J., Choi, J., Hong, J. S., & Park, K. R. (2020). Finger-Vein Recognition based on Densely Connected Convolutional Network using Score-Level Fusion with Shape and Texture Images. IEEE Access, 8, 96748-96766.

Park, K. R. (2011). Finger Vein Recognition by Combining Global and Local Features based on SVM. Computing and Informatics, 30(2), 295-309.

Prabu, A. J., & Bai, S. C. (2017). A Biometric Recognition System for Human Identification Using Finger Vein Patterns. International Journal of Emerging Trends in Engineering and Development, 2(7).

Qin, H., & El-Yacoubi, M. A. (2017). Deep Representation based Feature Extraction and Recovering for Finger-Vein Verification. IEEE Transactions on Information Forensics and Security, 12(8), 1816-1829.

Qin, H., & Wang, P. (2019). Finger-Vein Verification Based on LSTM Recurrent Neural Networks. Applied Sciences, 9(8), 1687.

Radhakrishnan, S., & Baskar, V. (2014). Finger Vein Authentication. International Journal of Engineering Research and Technology (IRJET), 10.

Radzi, S. A., Hani, M. K., & Bakhteri, R. (2016). Finger-Vein Biometric Identification using Convolutional Neural Network. Turkish Journal of Electrical Engineering and Computer Sciences, 24(3), 1863-1878.

Ren, H., Sun, L., Guo, J., Han, C., & Wu, F. (2021). Finger Vein Recognition System with Template Protection based on Convolutional Neural Network. Knowledge-based systems, 227, 107159.

Ronneberger, O., Fischer, P., & Brox, T. (2015). U-NET: Convolutional Networks for Biomedical Image Segmentation. In Medical Image Computing and Computer-Assisted Intervention–MICCAI 2015: 18th International Conference, Munich, Germany, October 5-9, 2015, Proceedings, Part III 18 (pp. 234-241). Springer International Publishing.

Rosdi, B. A., Mukahar, N., & Han, N. T. (2021). Finger Vein Recognition using Principle Component Analysis and Adaptive K-Nearest Centroid Neighbour Classifier. International Journal of Integrated Engineering, 13(1), 177-187.

Rosdi, B. A., Shing, C. W., & Suandi, S. A. (2011). Finger Vein Recognition using Local Line Binary Pattern. Sensors, 11(12), 11357-11371.

Roza, W. A., Kassim, J. M., & Abdullah, S. N. H. S. (2019). Finger Vein Recognition using Straight Line Approximation based on Ensemble Learning. International Journal of Advanced Computer Science and Applications, 10(1).

Sager, C., Janiesch, C., & Zschech, P. (2021). A Survey of Image Labelling for Computer Vision Applications. Journal of Business Analytics, 4(2), 91-110.

Shakil, S., Arora, D., & Zaidi, T. (2023). An Optimal Method for Identification of Finger Vein using Supervised Learning. Measurement: Sensors, 25, 100583.

Sharma, S., & Lohchab, S. (2021). Personal Authentication using Finger Vein Biometric Technology with Implementation of Transfer Learning CNN Model. In Proceedings of the International Conference on Advances in Management Practices (ICAMP 2021).

Shazeeda, S., & Rosdi, B. A. (2019). Finger Vein Recognition using Mutual Sparse Representation Classification. IET Biometrics, 8(1), 49-58.

Shen, J., Liu, N., Xu, C., Sun, H., Xiao, Y., Li, D., & Zhang, Y. (2021). Finger Vein Recognition Algorithm based on Lightweight Deep Convolutional Neural Network. IEEE Transactions on Instrumentation and Measurement, 71, 1-13.

Shorten, C., & Khoshgoftaar, T. M. (2019). A Survey on Image Data Augmentation for Deep Learning. Journal of big data, 6(1), 1-48.

Sidiropoulos, G. K., Kiratsa, P., Chatzipetrou, P., & Papakostas, G. A. (2021). Feature Extraction for Finger-Vein-Based Identity Recognition. Journal of Imaging, 7(5), 89.

Simonyan, K., & Zisserman, A. (2014). Very Deep Convolutional Networks for Large-Scale Image Recognition. arXiv preprint arXiv:1409.1556.

Song, J. M., Kim, W., & Park, K. R. (2019). Finger-Vein Recognition Based on Deep Densenet using Composite Image. IEEE Access, 7, 66845-66863.

Sun, Q., & Luo, X. (2022). A New Image Recognition Combining Transfer Learning Algorithm and Mobilenet V2 Model for Palm Vein Recognition. In 2022 4th International Conference on Frontiers Technology of Information and Computer (ICFTIC) (pp. 559-564). IEEE.

Tahir, A. A., & Mustafa, A. A. (2022). Improving the Performance of Finger Vein Recognition using the Local Histogram Concatenation of Image Descriptors. International Journal of Pattern Recognition and Artificial Intelligence, 36(14), 2256020.

Tao, Z., Zhou, X., Xu, Z., Lin, S., Hu, Y., & Wei, T. (2021). Finger-Vein Recognition using Bidirectional Feature Extraction and Transfer Learning. Mathematical Problems in Engineering, 2021(1), 6664809.

Thilagavathy, T., & Siruba, K. (2014). Personal Verification Through Finger Vein Pattern Recognition using Support Vector Machine. International Journal of Applied Science and Engineering, 2(1), 13-20.

Wang, K. Q., Khisa, A. S., Wu, X. Q., & Zhao, Q. S. (2012). Finger Vein Recognition using LBP variance with Global Matching. In 2012 International conference on wavelet analysis and pattern recognition (pp. 196-201). IEEE.

Wang, Xian, Huabin Wang, Ying He, Yijun Ding, and Liang Tao (2019). Novel Algorithm for Finger Vein Recognition based on Inception-Resnet Module. In Eleventh International Conference on Digital Image Processing (ICDIP 2019), vol. 11179, pp. 367-375. SPIE.

Wang, Y., Shi, D., & Zhou, W. (2022). Convolutional Neural Network Approach based on Multimodal Biometric System with Fusion of Face and Finger Vein Features. Sensors, 22(16), 6039.

Weng, L., Li, X., & Wang, W. (2020). Finger Vein Recognition Based on Deep Convolutional Neural Networks. In 2020 13th International Congress on Image and Signal Processing, Bio Medical Engineering and Informatics (CISP-BMEI) (pp. 266-269). IEEE.

Xi, X., Yang, G., Yin, Y., & Yang, L. (2014). Finger Vein Recognition Based on the Hyper Information Feature. Optical Engineering, 53(1), 013108-013108.

Xi, X., Yang, L., & Yin, Y. (2017). Learning Discriminative Binary Codes for Finger Vein Recognition. Pattern Recognition, 66, 26-33.

Xie, C., & Kumar, A. (2017). Finger Vein Identification using Convolutional Neural Network and Supervised Discrete Hashing. Deep Learning for Biometrics, 109-132.

Yang, H., Fang, P., & Hao, Z. (2020). A GAN-based Method for Generating Finger Vein Dataset. In Proceedings of the 2020 3rd International Conference on Algorithms, Computing and Artificial Intelligence (pp. 1-6).

Yang, L., Yang, G., Wang, K., Hao, F., & Yin, Y. (2021). Finger Vein Recognition via Sparse Reconstruction Error Constrained Low-Rank Representation. IEEE Transactions on Information Forensics and Security, 16, 4869-4881.

Yang, W., Hui, C., Chen, Z., Xue, J. H., & Liao, Q. (2019). FV-GAN: Finger Vein Representation using Generative Adversarial Networks. IEEE Transactions on Information Forensics and Security, 14(9), 2512-2524.

Yang, W., Qin, C., & Liao, Q. (2012). Visual Information Processing Lab, Tsinghua University, THU-FVFDT1: Finger Vein and Finger Dorsal Texture Database, https://www.sigs.tsinghua.edu.cn/labs/vipl/thu-fvfdt.html.

Yilong Yin, Lili Liu, and Xiwei Sun. SDUMLA-HMT: A Multimodal Biometric Database,The 6th Chinese Conference on Biometric Recognition (CCBR 2011), LNCS 7098, pp. 260-268, Beijing, China, 2011

Yu, C. B., Qin, H. F., Cui, Y. Z., & Hu, X. Q. (2009). Finger-Vein Image Recognition Combining Modified Hausdorff Distance with Minutiae Feature Matching. Interdisciplinary Sciences: Computational Life Sciences, 1, 280-289.

Zeng, J., Chen, Y., Zhai, Y., Gan, J., Feng, W., & Wang, F. (2019). A Novel Finger-Vein Recognition Based on Quality Assessment and Multi-Scale Histogram of Oriented Gradients Feature. International Journal of Enterprise Information Systems (IJEIS), 15(1), 100-115.

Zhang, J., Lu, Z., Li, M., & Wu, H. (2019). GAN-Based Image Augmentation for Finger-Vein Biometric Recognition. IEEE Access, 7, 183118-183132.

Zhang, X., & Wang, W. (2020, September). Finger Vein Recognition Method based on GLCM-HOG and SVM. In 2020 IEEE 3rd International Conference on Information Systems and Computer Aided Education (ICISCAE) (pp. 698-701). IEEE.

Zhang, Z., & Wang, M. (2022). A Simple and Efficient Method for Finger Vein Recognition. Sensors, 22(6), 2234.

Zhang, Z., Chen, G., Zhang, W., & Wang, H. (2023). Finger Vein Recognition based on ResNet with Self-Attention. IEEE Access.

Zhang, Z., Zhou, Z., Yang, X., Meng, H., & Wu, G. (2023). Convolutional Neural Network based on Multi-Directional Local Coding for Finger Vein Recognition. Information Sciences, 623, 633-647.

Zhou, L. (2023). Finger Vein Recognition Technology: Principles, Applications, and Future Prospects. International Journal of Biology and Life Sciences, 3(2), 45-48.

PUBLICATIONS

1. Amitha Mathew, Amudha P. (2024). Enhancing Finger Vein Authentication through Deep Learning: A Comparative Study of U-Net and Sequential Models. *Journal of Advanced Research in Applied Sciences and Engineering Technology*, 47(1), 230-243. https://doi.org/10.37934/araset.47.1.230243 (SCOPUS)

2. Amitha Mathew, Amudha P. (2024). Improved Finger Vein Recognition Using Generative Adversarial Network and Transfer Learning. *Journal of Nanoelectronics and Optoelectronics*, 19(10), 1053–1062 https://doi.org/10.37934/araset.47.1.230243 (SCIE)

3. Amitha Mathew, Amudha P. (2024). Motion Tolerant Finger Vein Authentication using Deep Learning Techniques. *International Journal of Intelligent Systems and Applications in Engineering*, *12*(4), 2407 – 2413. https://ijisae.org/index.php/IJISAE/article/view/6628(SCOPUS)

Avinashilingam Institute for HomeScience and Higher Education for Women

(Deemed to be University Estd. u/s 3 of UGC Act 1956, Category 'A' by MHRD
Re-accredited with A++ Grade by NAAC. CGPA 3.65/4, Category I by UGC
Coimbatore - 641 043, Tamil Nadu, India

Appendix I.2

(Item No 5 of Check List) Details of Research Publications

S.No	Article	Journal	Other Details Vol/No/Page No/ Year	Published in UGC-CARE / Scopus Indexed/ Web of Science
1	Enhancing Finger Vein Authentication Through deep learning: A Comparative study of U-NET and Sequential models	Journal of Advanced Research in Applied Sciences and Engineering Technology	Vol. 47 Issue: 1 Page No: 230-243 (2025) https://doi.org/10.37934/araset.47.1.230243	Scopus Indexed
2	Improved Finger Vein Recognition Using Generative Adversarial Network and Transfer Learning	Journal of Nanoelectronics and Optoelectronics	Accepted	Web of Science Indexed

*Proof of list of Journals from Internet to be attached along with copies of reprints.

Scholar : Amitha Mathew

Supervisor : 4/10/24 (Dr. P. AMUDHA)

4/10/24 Checked By: 4/10/24

HoD/Dean of Respective School

The scholar Miss. Amitha Mathew (18PHEOP002) has published her research articles in the following journals:

1. Journal of Advanced Research in Applied Sciences and Engineering Technology - indexed in Scopus and
2. Journal of Nanoelectronics and optoelectronics - indexed in Web of Science - Science Citation Index Expanded.

This may be considered.

J. Th[illegible]
11.09.24.
Asst. Librarian.

SEMARAK ILMU PUBLISHING

Journal of Advanced Research in Applied Sciences and Engineering Technology

Journal homepage: https://semarakilmu.com.my/journals/index.php/applied_sciences_eng_tech/index
ISSN: 2462-1943

Enhancing Finger Vein Authentication through Deep Learning: A Comparative Study of U-Net and Sequential Models

Amitha Mathew[1,*], P. Amudha[2]

[1] Department of Computer Science and Engineering, Avinashilingam Institute for Home Science and Higher Education for Women, Coimbatore, India
[2] Department of Computer Science and Engineering, Avinashilingam Institute for Home Science and Higher Education for Women, Coimbatore, India

ARTICLE INFO

Article history:
Received 22 August 2023
Received in revised form 20 April 2024
Accepted 23 May 2024
Available online 20 June 2024

Keywords:
Biometric; Deep learning; Finger vein authentication; Sequential model; U-Net

ABSTRACT

The use of finger veins as biometric authentication is becoming increasingly popular. However, low-quality finger vein images pose challenges, necessitating innovative approaches for accurate authentication. This research investigates the potential of deep learning techniques in addressing this issue, focusing on two prominent architectures: U-Net and the proposed Sequential Model. The study conducts a comparative analysis of the performance of these models in low-quality finger vein image authentication scenarios. U-Net, known for its image segmentation capabilities, is explored for feature extraction, while the Sequential Model, incorporating a modified VGG16 architecture, brings temporal context through LSTM layers. The research presents an in-depth evaluation of both models based on accuracy, recall, precision, and other relevant metrics. The findings shed light on the suitability of each approach for enhancing the reliability of finger vein authentication in challenging data quality contexts.

1. Introduction

A finger vein authentication system uses patterns of veins beneath the skin to verify an individual's identity. A unique vein pattern on each finger makes it a secure biometric authentication method, even if they are identical twins. Since the veins are inherent to our bodies, they cannot be faked or stolen. In addition, the finger vein authentication system, being a contactless authentication system, reduces the spread of epidemic diseases compared to the widely used fingerprint system. It is not necessary to re-register finger vein patterns during the adult years because they remain relatively constant, and they are less affected by age or physical condition. Changes in the weather or an individual's physical condition have less effect on finger veins.

Due to hygiene-related issues, contactless biometrics like finger veins have been predicted to serve best in the future. Biometrics based on finger veins can be used in a variety of scenarios. The

* *Corresponding author.*
E-mail address: amithamathew669@gmail.com

https://doi.org/10.37934/araset.47.1.230243

finger vein biometric authentication method allows access to various networks, web applications, web portals etc. without the need to remember long passwords for each application. Furthermore, it can be used in the banking domain for credit card authentication, and online transactions to improve security and customer convenience. In addition to reducing the time it takes to log in, and eliminating the need to type usernames and passwords, it also reduces the financial burden of password resets. Physical access control can also be made possible by finger vein authentication including passenger verification at airports, attendance tracking, home security, school security, building access, automobile security, etc. This helps to avoid problems associated with lost, fraudulent, or stolen keys, cards, etc. [1].

The haemoglobin in veins changes colour when exposed to infrared light or visible light, which can be captured with an infrared scanner or a visible light camera. This can be utilised for acquiring finger vein images for enrolment and authentication [2].

In this study initially, a U-Net [3,4] architecture was employed for finger vein recognition. As authentication mechanisms are intended to grant access to legitimate individuals and prevent unauthorized imposters, achieving an accuracy close to 100% is crucial. To attain this goal a novel Sequential model is proposed in this study, which was able to achieve an accuracy close to 100. In the sequential model, a modified VGG16 architecture was used by removing the final fully connected layers and incorporating a time-distributed layer, an LSTM layer, and a dense layer instead. This innovative architecture significantly enhances the accuracy and reliability of the finger vein authentication system. This method works well with high-quality finger vein images as well since it was demonstrated with low-quality finger vein images.

The paper's structure is outlined as follows: Section 2 presents a discussion of related literature. Section 3 details the finger vein authentication system. The configuration of experiments and deep learning architectures is explained in Section 4. Section 5 evaluates the outcomes of comparative tests, and the paper concludes with Section 6.

2. Related Works

Deep learning approaches have shown promise in enhancing the effectiveness of finger vein recognition. However, they have limitations and face several challenges. While some systems propose robustness against noise and deformation [5], others claim to handle misalignment and shading [6], and some aim to address image quality variations [7]. However, none of these solutions are universally robust, and the performance may suffer in real-world scenarios with multiple challenges simultaneously.

Many of the proposed systems rely on deep learning models, such as CNNs [5,8], FCNNs [9], and capsule models [10]. However, obtaining a diverse and extensive dataset with image-level annotations is challenging, leading to limited training samples, and potentially affecting the system's performance. The absence of pixel-level texture labels in public finger vein databases further hinders the development of accurate recognition models. The multistage transfer learning used to address the lack of labelled training samples introduces dependencies on pre-trained models, potentially limiting the system's adaptability to new environments [11]. By combining deep learning, specifically semantic segmentation CNNs, with automatic label generation, Jalilian *et al.,* improved finger vein recognition performance compared to classical techniques. Their study demonstrates that certain FCN architectures, such as U-Net and RefineNet, outperform classical methods and highlight the significance of label quality [12].

The recognition issues caused by misalignment and illumination variations by introducing a biometric system. However, the integration of multiple sensors and the complexity of deep convolutional neural networks can increase the computational burden and raise practical implementation challenges [13]. Tamilarasi *et al.,* used convolutional and recurrent neural networks in capturing temporal information and has shown promising results. But the sensitivity to hand movements and variations in behaviour can still affect the system's identification accuracy [14]. While the capsule model proposed by Yagoub, *et al.,* outperforms certain ANN models, its implementation is more complex and resource-intensive, making it less suitable for certain applications with limited computational resources [15].

Several proposed systems rely on preprocessing techniques, such as bias field correction, spatial attention mechanisms, and feature block fusion. These techniques may be sensitive to parameter tuning and might not be robust to unseen data [16]. The challenge of limited public finger vein datasets for training effective convolutional neural networks (CNNs) utilizing a pre-trained CNN model to extract vein features. Chiranjeevi, *et al.,* proposed a light weight deep-learning framework for real-time sentiment analysis, addressing the computational and dataset limitations associated with neural networks. They also mention the need for improved preprocessing to address rotation and displacement issues, addressing the insufficient number of training samples, and refining the topological structure for a more complete end-to-end framework [17].

While deep learning approaches hold great promise for enhancing finger vein recognition systems, the existing solutions face challenges in robustness, data availability, and integration complexity, reliance on preprocessing techniques and transfer learning, as well as performance issues. Addressing these disadvantages is essential for developing efficient and reliable authentication systems based on finger vein recognition. Deep learning-based authentication is influenced by a variety of factors. These factors include the learning architecture, the training strategies, and the feature extraction methods.

3. Architecture of Deep Learning-Based Finger Vein Recognition System

A finger vein recognition system using a deep model includes two phases, model generation and recognition:

i. Model Generation Phase: The steps involved in the model generation phase are data collection, preprocessing, data augmentation (if required), model training, and model evaluation. The first step is to collect a database containing finger vein images. Then pre-process the dataset by normalizing the images, crop vein part of the image, and resizing the images to improve the quality of the input data. The dataset size can be increased by performing data augmentation techniques such as translation, rotation, flipping etc. The augmented images are divided into training, validation, and testing sets. Design a deep learning model architecture suitable for finger vein recognition. Utilize an appropriate optimizer to optimize the model's weights based on the training data. Determine a loss function to train the model and monitor the training using metrics such as accuracy or loss. The performance of the model should be evaluated using a separate data set that was not used during the model's training or validation. Assess the accuracy of the model by examining metrics such as accuracy, precision, recall, and F1 score. Once the model has achieved satisfactory performance, deploy it in a production environment where it can be utilized for real-time finger vein recognition.

ii. Recognition Phase: During the recognition phase, the trained finger vein model takes the image of a person's finger vein as an input and outputs a prediction of whether the image belongs to the individual whose finger vein is being authenticated or not. This involves the following steps. The input image is pre-processed to normalize, crop, and resize the image to match the input size of the trained model. The pre-processed image is fed into the model that has been trained. Based on the possible classes, a probability distribution is computed. If the probability score is above the threshold, the user is accepted as authenticated, and if it falls below the threshold, the user is rejected. The threshold for the probability score in finger vein authentication is typically set by the system administrator or the developer of the system based on the desired level of security, rate of false acceptances and rejections. Figure 1 shows the architecture of the finger vein authentication system employing deep learning techniques.

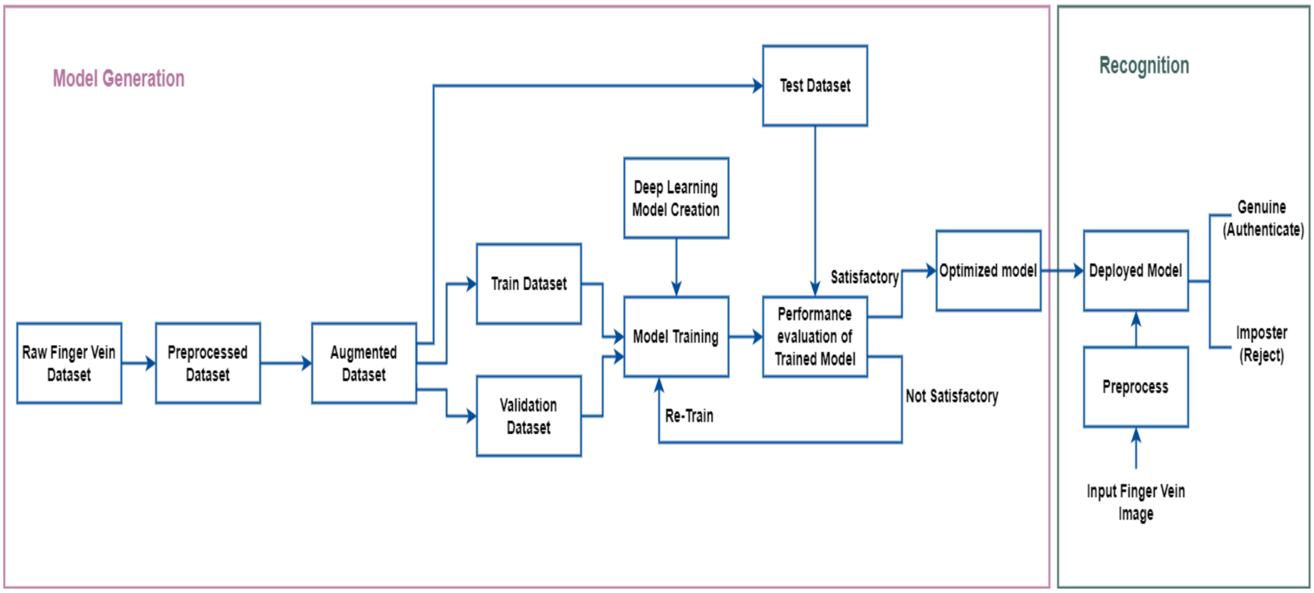

Fig. 1. Finger vein authentication system

4. Experimental Setup

4.1 Database

This study uses the SDUMLA-HMT finger vein database captured by Shandong University which contains finger vein images of 106 persons. The ring, middle and index fingers of the right and left hand of all these persons are captured repeatedly 6 times which adds up to 3816 images. The images are of size 320*240 and are available in bmp format. The images are captured without using any guide bar. Since the images are prone to misalignments and shading, we can consider this to be a low-quality finger vein database.

4.2 Pre-Processing

The vein region is extracted from the captured image using a set of pre-processing operations. First the contrast of the original image was enhanced through histogram equalization. Then, the intensity values are blurred using bilateral filtering, which maintains sharp intensity changes while blurring the intensity values similar to the central pixel. Then, the image is divided horizontally, and separate masks are created for each half. The “canny edge detection method” is used to separate the region of interest (ROI), which contains the actual finger veins. Then dilation and erosion operations are applied to ROI to refine it [20]. ROI is transformed into an image with dimensions of 200x200. The original images from the “SDUMLA-HMT” database and the pre-processed and ROI extracted images are shown in Figure 2.

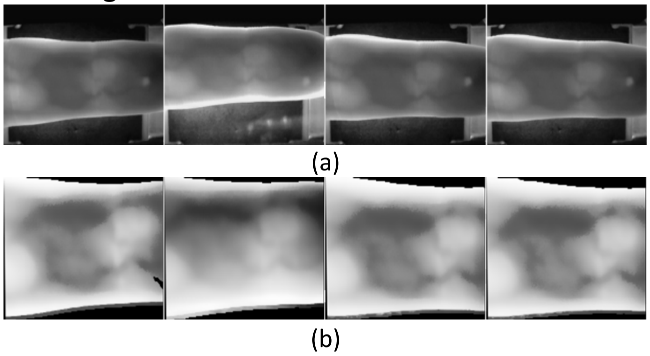

Fig. 2. (a) Original images from the "SDUMLA-HMT" finger vein database (b) Images after preprocessing and ROI extraction

4.3 Data Augmentation

In image augmentation, different transformations are applied to original images, resulting in multiple transformed copies. It helps in increasing the diversity of the dataset and can lead to better generalization and improved performance of machine learning models [18,19]. Depending on the augmentation technique, each copy differs in certain aspects. The dataset comprises only four images for each individual, which is insufficient for training a deep-learning model. To address this limitation, we employ various transformations such as shifting, rotation, brightness adjustments, and zooming [20].

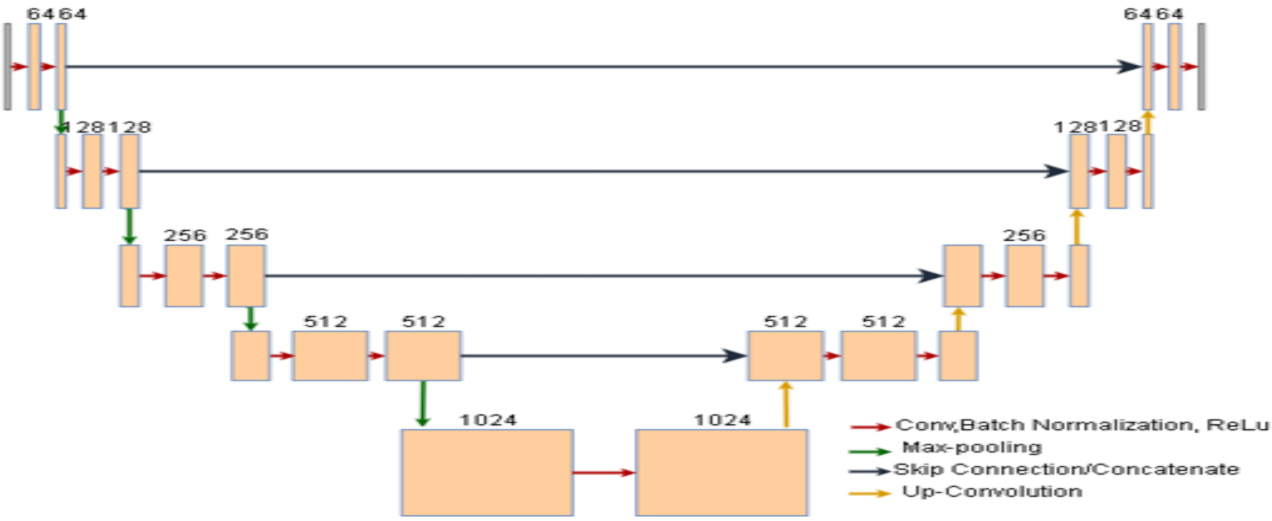

Fig. 3. Architecture of U-Net

These augmentation techniques can be mathematically denoted as follows:

Shifting or Translation: x=x+dx (1)

y' = y+dy (2)

In Eq. (1), x, x' are the original and shifted horizontal pixel coordinates, respectively. In Eq. (2) y, y' are the original and shifted vertical pixel coordinates, respectively. dx, dy represents the shift in x, y directions, respectively. The value of dx and dy may range from [-10,10] pixels.

Rotation: x' = x*cos(θ) - y*sin(θ) (3)

y= x*sin(θ)+ y*cos(θ) (4)

In Eq. (3), ‘x’, ‘x'’ corresponds to the original and rotated horizontal pixel coordinates, respectively. Similarly in Eq. (4) ‘y’, ‘y'’ refer to the original and rotated vertical pixel coordinates, respectively. θ represents the angle of rotation. The value of θ may range from [-15, 15].

Brightness adjustment: np=op+bf (5)

In Eq. (5) np is the new pixel value, op is the old pixel value and bf is the brightness factor which may vary between [-0.2, 0.2].

Zooming or Scaling: x' = x * sf (6)

y' = y * sf (7)

In Eq. (6), x, x' are the old and new horizontal pixel coordinates respectively. In Eq. (7) y, y' are the old and new vertical pixel coordinates respectively, and sf is the scaling factor which lies between [0.8,1.2].

By using the above augmentation techniques 40 augmented images per finger per person are generated. Hence a total of 240 images were available for each person and this can be used as the sequence of images which are to be input to the model. The augmented images are shown in Figure 4.

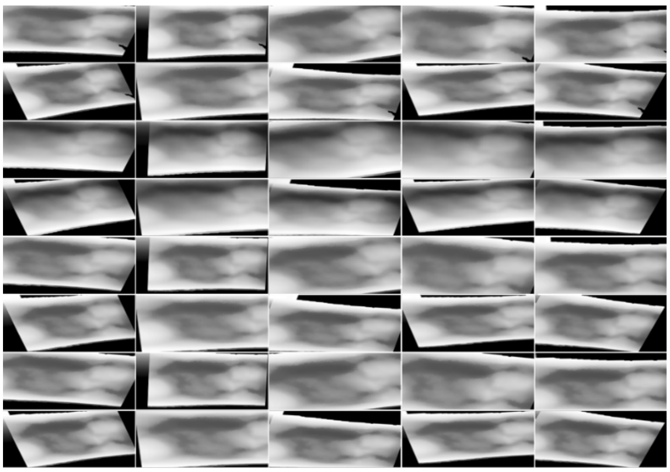

Fig. 4. Images after applying augmentation techniques

4.4 U-Net

U-Net can be used for computer vision applications, including biometric recognition. Feature extraction and matching can be performed with U-Net. The network's ability to learn to identify and extract unique patterns and features present in finger vein images can be used for matching and authentication [21].

U-Net architecture consists of two paths: a contracting one and an expanding one. Information from the input image is obtained through the contracting path, which involves extracting both context and features, while the expanding path up samples the features and produces a segmentation mask. In finger vein recognition, the segmentation mask can be used to identify and extract vein patterns and features.

The structure of the model is described below. Several layers undergo encoding and decoding via a pair of convolutional layers, each accompanied by Batch Normalization and activated by ReLU. After a convolutional block, a max-pooling block follows within the encoder segment. Through max pooling, the spatial dimensions can be reduced, and while augmenting the count of feature channels. The decoder block performs up-sampling using Conv2DTranspose to increase the spatial dimensions and concatenates it with the corresponding skip features from the encoder block. The concatenated features are then processed by a convolution block. The encoder blocks capture hierarchical features at different scales, while the decoder blocks use skip connections to help recover spatial information lost during max pooling.

The optimizer used is Adam optimizer which uses regularization technique to prevent overfitting. The employed loss function is “binary cross entropy” which can be defined as follows.

$$\text{Binary Cross Entropy} = -\frac{1}{N}\sum_{i-1}^{N}(\mathrm{Y} * \log(\mathrm{p(y)}) \ + 1 - \mathrm{Y} * \log(1 - \mathrm{p(y)})) \quad (8)$$

In Eq. (8), N corresponds to total count of instances (persons), Y represents class 1, P(Y) stands for the probability associated with class 1, while 1-Y refers to class 0, 1-P(Y) signifies the probability for class 0. Figure 4 shows the details of U-Net architecture. The implementation details of different layers of the U-Net model with the number of parameters are shown in Figure 5.

It is necessary to train the U-Net to learn to extract unique vein patterns and features, to use it for finger vein recognition. During testing, an input finger vein image can be passed through the trained U-Net, which would extract the vein patterns and features and produce a segmentation mask. This mask can then be used for matching and identification [22].

batch_normalization	(none, 128,128,64)	256	conv2d[0][0]
activation	(none, 128,128,64)	0	batch_normalization[0][0]
conv2d_1	(none, 128,128,64)	36928	activation [0][0]
batch_normalization_1	(none, 128,128,64)	256	conv2d_1[0][0]
activation_1	(none, 128,128,64)	0	batch_normalization_1[0][0]
max_pooling2d	(none, 64,64,64)	0	activation_1[0][0]
conv2d_2	(none, 64,64,128)	73856	max_pooling2d[0][0]
batch_normalization_2	(none, 64,64,128)	512	conv2d_2[0][0]
activation_2	(none, 64,64,128)	0	batch_normalization_2[0][0]
conv2d_3	(none, 64,64,128)	147584	activation_2[0][0]
batch_normalization_3	(none, 64,64,128)	512	conv2d_3[0][0]
activation_3	(none, 64,64,128)	0	batch_normalization_3[0][0]
conv2d_12	(none, 128,128,64)	73792	activation_11[0][0]
batch_normalization_12	(none, 128,128,64)	256	conv2d_12[0][0]
activation_12	(none, 128,128,64)	0	batch_normalization_12[0][0]
conv2d_transpose_3	(none, 256,256,32)	8224	activation_12[0][0]
concatenate_3	(none, 256,256,64)	0	conv2d_transpose_3[0][0]
conv2d_13	(none, 256,256,32)	18464	concatenate_3[0][0]
batch_normalization_13	(none, 256,256,32)	128	conv2d_13[0][0]
activation_13	(none, 256,256,32)	0	batch_normalization_13[0][0]
conv2d_14	(none, 256,256,32)	9248	activation_13[0][0]
batch_normalization_14	(none, 256,256,32)	128	conv2d_14[0][0]
activation_14	(none, 256,256,32)	0	batch_normalization_14[0][0]
conv2d_15	(none, 256,256,1)	33	activation_14[0][0]

Fig. 5. Details of different layers of U-Net Model

4.5 The Proposed -Sequential Model

The proposed sequential model uses VGG16 as a feature extractor, followed by a Time Distributed layer, LSTM layer, and dense layer for classification. The images in the finger vein dataset are organized into sequences, where each sequence contains a series of finger vein images for an individual.

VGG16 architecture is used due to its strong feature extraction capabilities and the ability to learn intricate patterns from images. With VGG16 architecture, the finger veins can be extracted more effectively for proper finger vein biometric authentication because of its strong feature extraction capabilities. In this architecture, 13 convolutional layers are followed by ReLU activation for each of them, using 3x3 filters and stride 1 with zero padding. Max pooling layers with a 2x2 window and stride 2 are applied after every two convolutional layers, reducing spatial dimensions while preserving key features. The fully connected layers from VGG16 architecture are removed. For each input image, a fixed-size feature vector is generated using the convolutional layers of VGG16 [23].

A Time Distributed layer with a flatten layer inside it is used to treat each frame of the finger vein sequence separately, while the flatten layer reshapes the data for the subsequent LSTM layer. This layer will create a sequence of feature vectors that represents the temporal information for the LSTM [24]. Figure 6 illustrates the structure of the sequential model put forth in this study.

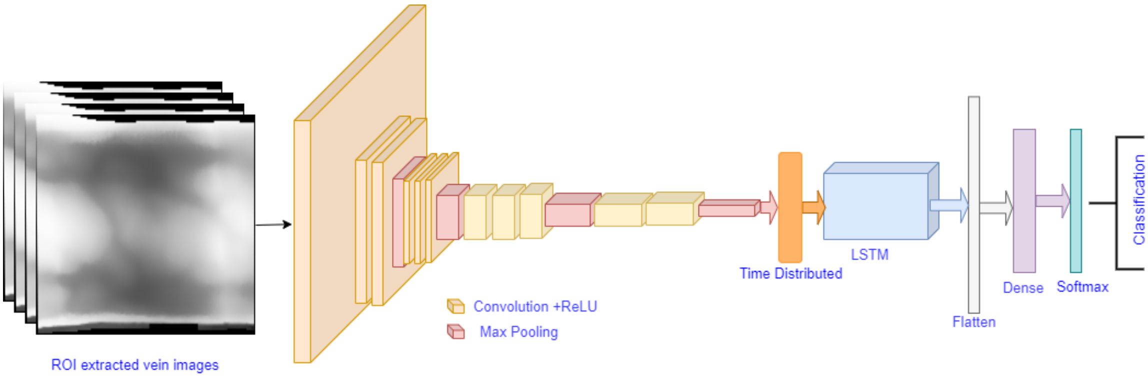

Fig. 6. The proposed Sequential model for finger vein authentication

The LSTM model will take in this sequence of feature vectors as input and learn to capture temporal dependencies between vectors. An LSTM layer with the 32 hidden unit neurons and a flatten layer is then added. A Dense layer with 106 neurons representing the 106 classes (person) and a SoftMax activation function is added for classification. The model is trained for 25 epochs, and it could produce an accuracy of 99.76%. Figure 7 displays distinct layers within the Sequential model along with their corresponding parameter counts.

Layer	Output Shape	Param#
VGG16 (Functional)	(None, 7, 7, 512)	14714688
Time Distributed	(None, 7, 7, 512)	0
LSTM	(None, 7, 100)	245200
Flatten	(None,700)	0
Dense	(None,106)	74206

Fig. 7. Details of different layers of Sequential Model

5. Results and Discussion

Table 1 presents a comparison of various parameters utilized in both models. The loss function used in both cases is binary cross entropy. The optimizer used in U-Net is Adam with an initial learning rate set as 0.001 and the Sequential model utilizes the optimizer RMS prop with the initial learning rate set as 0.0001. Adam combines the features of both RMSprop and momentum-based approaches whereas RMS prop uses second order momentum only for adjusting the learning rates. RMSprop has fewer hyperparameters which makes it easier to tune and use.

It is important to note that the U-Net model underwent a lengthy training period of 40 epochs, during which time it consistently achieved an accuracy of 95.7% from the 20th epoch to the 40th epoch. The sequential model, in contrast, provided a significantly higher level of performance by achieving an accuracy of 99.76% across 25 epochs, outperforming the U-Net model by a considerable margin by training through 25 epochs. Being a biometric finger vein authentication technique, it is crucial to achieve this high level of accuracy to authenticate genuine and imposter in the real time scenarios.

Table 1
Comparison of parameters in U-Net and Sequential Model

	U-Net	Sequential Model
Loss function	"Binary Cross Entropy"	"Binary Cross Entropy"
Optimizer	"Adam Optimizer"	"RMSprop optimizer"
Initial Learning Rate	1e-3	1e-4
No of Epochs Trained	40	25
Evaluation Metric	Accuracy 95.7%	Accuracy 99.7%

A comparison of the count of parameters in both models are displayed in Table 2. Total Parameters refer to both trainable and non-trainable parameters, including weights and biases. Trainable Parameters are a subset of total parameters that undergo learning and updates during the training process to optimize the model. Non-trainable parameters encompass the remaining parameters that remain unaltered during the training process.

The U-Net model has a relatively large number of total parameters, indicating that it is a complex model with a significant number of learnable weights and biases. Around 31,793,480 of these parameters are trainable, which means they can be updated during training to enhance the model's efficiency. The remaining 5,440 parameters are not trainable, whose values are fixed throughout training.

The Sequential model has a total parameter count of 15,034,094, which is smaller than the U-Net model. The trainable parameters amount to 319,406, while the non-trainable parameters are much larger, at 14,714,688.

Table 2
Comparison of parameters in U-Net and Sequential model

	Total Parameters	Trainable Parameters	Non-Trainable Parameters
U-Net	31,798,920	31,793,480	5,440
Sequential Model	15,034,094	319,406	14,714,688

The large count of parameters to be trained in the U-Net model indicates a more complex model. The smaller count of non-trainable parameters in the Sequential model suggests faster training and resource efficient operation.

Figure 8 shows the accuracy and loss graph for the U-Net model. The plot indicates that the model has been converged with a validation accuracy of 95.7% as the accuracy remains stable from 18th epoch to 40th epoch which indicates that further optimization may not lead to significant improvement in the accuracy.

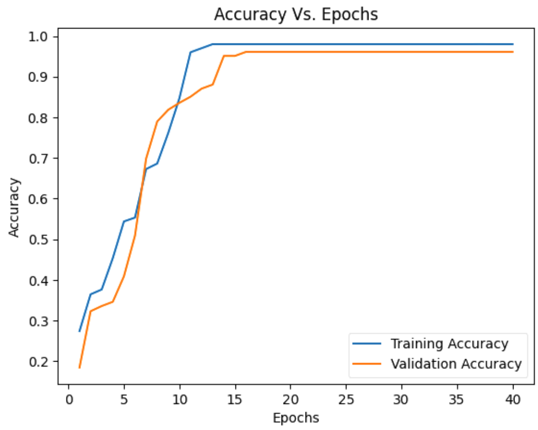

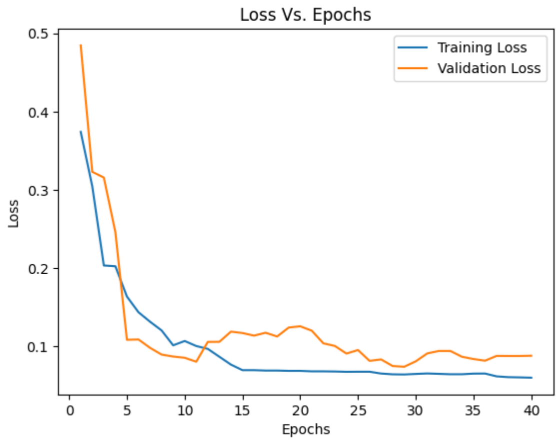

(a) (b)

Fig. 8. U-Net Model: (a) Accuracy Vs Number of Epochs plot (b) Loss Vs Number of Epochs plot

The accuracy and loss graph for the Sequential model is plotted in Figure 9. The plot indicates that the model has been converged with a validation accuracy of 99.7%.

An authentication system's effectiveness and reliability can be evaluated by considering the evaluations metrics like accuracy, Precision, Recall, F1-Score, Kappa Score and Matthews Correlation Coefficient as defined below.

Accuracy is computed by dividing the count of accurate predictions by the total number of predictions made.

$$\text{Accuracy} = \frac{True\ Positives + True\ Negatives}{Total\ Predictions} \tag{9}$$

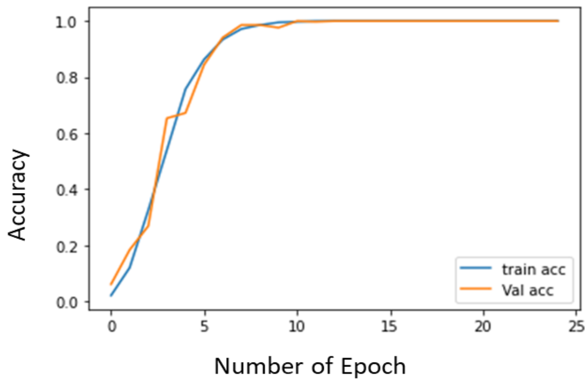

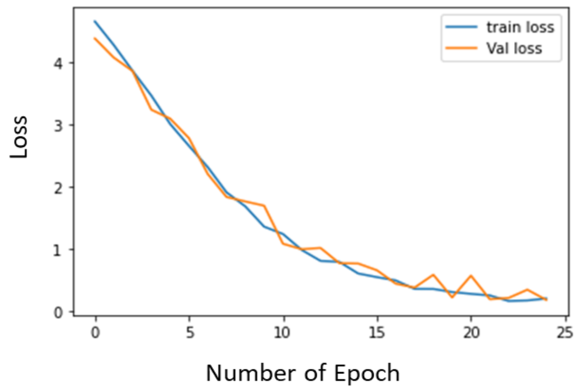

(a) (b)

Fig. 9. U-Net Model: (a) Accuracy Vs Number of Epochs plot (b) Loss Vs Number of Epochs plot

Precision measures the correctly predicted true positives to the total positive predictions.

$$\text{Precision} = \frac{True\ Positives}{Total\ Positive\ \ Predictions} \tag{10}$$

The proportion of correctly predicted positive instances relative to the total number of actual positive instances is referred to as recall, sensitivity, or true positive rate.

$$\text{Recall} = \frac{True\ Positives}{True\ Positives + False\ Negatives} \tag{11}$$

In the F1-Score, precision and recall are combined to form a harmonic mean.

$$\text{F1-Score} = \frac{2(Precision * Recall)}{Precision + Recall} \tag{12}$$

The Kappa Score, also referred to as Cohen's Kappa Coefficient, quantifies the agreement between predicted and actual labels, considering the potential for random agreement. It provides insight into the quality and reliability of the model.

$$\text{Kappa} = \frac{(Po - Pe)}{(1 - Pe)} \tag{13}$$

"Po" denotes the fraction of observed agreement and "Pe" denotes the fraction of expected agreement by chance.

The Matthews Correlation Coefficient evaluates the effectiveness of binary classifications, considering true positives (TP), true negatives (TN), false positives (FP), and false negatives (FN).

$$\text{MCC} = \frac{(TP * TN - FP * FN)}{\sqrt{((TN + FN)(TP + FP)(TP + FN)\,(TN + FP))}} \tag{14}$$

Table 3 shows various metric values for the different deep learning models. The sequential model exhibits better performance compared to other models, suggesting its suitability for finger vein authentication.

Table 3
Comparison of evaluation metrics for U-Net and Sequential Model

	Accuracy	Precision	Recall	F1-Score	Kappa Score	Matthews Corrcoef
AlexNet [25]	0.7020	0.7010	0.9030	-	-	-
ResNet18 [24]	0.9713	0.9837	0.9587	-	-	-
VGGNet16 [24]	0.9710	0.9861	0.9554	-	-	-
VGG19 [25]	0.8757	0.88	0.78	-	-	-
U-Net	0.9571	0.9702	0.9750	0.973	0.664	0.973
Sequential	0.9976	0.9742	0.9976	0.986	0.989	0.990

The graphical representation of the basic evaluation metrics has been provided in Figure 10 for better comparison.

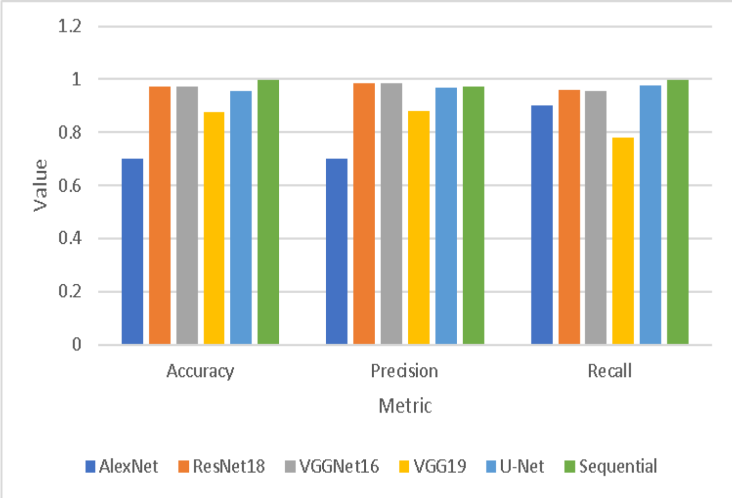

Fig. 10. Comparison of evaluation metric for different models

5. Conclusion

As the finger vein biometric authentication gains more importance in the scenario of contactless authentication system, the significance for accurate and reliable authentication is evident. This study addresses the challenges posed by low quality finger vein images through a comparative analysis of two deep learning architectures: U-Net and the proposed sequential model. The investigation brings out the capability of deep learning models to overcome the limitations of low-quality images. U-Net demonstrated its capacity to extract relevant features from noisy inputs, whereas the sequential model with modified VGG16 architecture and integration of LSTM layers introduced temporal context further enhancing accuracy and reliability. This research sheds light on the effectiveness of finger vein authentication using low quality images. The primary challenge faced in this work is the training time required to find an optimal architecture for achieving this accuracy, which could be improved by future researchers.

Acknowledgement
This research was not funded by any grant.

References
[1] Zayed, Hossam L., Heba M. Abdel Hamid, Yasser M. Kamal, and Abdel Halim A. Zekry. "A comprehensive survey on finger vein biometric." *Journal of Advances in Information Technology* 14, no. 2 (2023). https://doi.org/10.12720/jait.14.2.212-223
[2] Uhl, Andreas. "State of the art in vascular biometrics." *Handbook of Vascular Biometrics* (2020): 3-61. https://doi.org/10.1007/978-3-030-27731-4_1
[3] Wang, Peng, and Huafeng Qin. "Palm-vein verification based on U-Net." In *IOP Conference Series: Materials Science and Engineering*, vol. 806, no. 1, p. 012043. IOP Publishing, 2020. https://doi.org/10.1088/1757-899X/806/1/012043
[4] Htet, Aung Si Min, and Hyo Jong Lee. "Contactless Palm Vein Recognition Based on Attention-Gated Residual U-Net and ECA-ResNet." *Applied Sciences* 13, no. 11 (2023): 6363. https://doi.org/10.3390/app13116363
[5] Liu, Zhi, Yilong Yin, Hongjun Wang, Shangling Song, and Qingli Li. "Finger vein recognition with manifold learning." *Journal of Network and Computer Applications* 33, no. 3 (2010): 275-282. https://doi.org/10.1016/j.jnca.2009.12.006
[6] Hong, Hyung Gil, Min Beom Lee, and Kang Ryoung Park. "Convolutional neural network-based finger-vein recognition using NIR image sensors." *Sensors* 17, no. 6 (2017): 1297. https://doi.org/10.3390/s17061297

[7] Chawla, Bhavya, Shikhar Tyagi, Rupav Jain, Archit Talegaonkar, and Smriti Srivastava. "Finger vein recognition using deep learning." In *Proceedings of International Conference on Artificial Intelligence and Applications: ICAIA 2020*, pp. 69-78. Springer Singapore, 2021. https://doi.org/10.1007/978-981-15-4992-2_7
[8] Kharbas, Pratiksha, Arati Deshmukh, Siddhi Khalate, and Sumit Shinde. "Finger Vein Detection Based On Deep Learning."
[9] Jalilian, Ehsaneddin, and Andreas Uhl. "Finger-vein recognition using deep fully convolutional neural semantic segmentation networks: The impact of training data." In *2018 IEEE international workshop on information forensics and security (WIFS)*, pp. 1-8. IEEE, 2018. https://doi.org/10.1109/WIFS.2018.8630794
[10] Gumusbas, Dilara, Tulay Yildirim, Mustafa Kocakulak, and Nurettin Acir. "Capsule network for finger-vein-based biometric identification." In *2019 IEEE symposium series on computational intelligence (SSCI)*, pp. 437-441. Ieee, 2019. https://doi.org/10.1109/SSCI44817.2019.9003019
[11] Huang, Zhe, and Chengan Guo. "Robust finger vein recognition based on deep CNN with spatial attention and bias field correction." *International Journal on Artificial Intelligence Tools* 30, no. 01 (2021): 2140005. https://doi.org/10.1142/S0218213021400054
[12] Jalilian, Ehsaneddin, and Andreas Uhl. "Enhanced segmentation-CNN based finger-vein recognition by joint training with automatically generated and manual labels." In *2019 IEEE 5th international conference on identity, security, and behavior analysis (ISBA)*, pp. 1-8. IEEE, 2019. https://doi.org/10.1109/ISBA.2019.8778522
[13] Kalaivani, K., Pravin R. Kshirsagarr, J. Sirisha Devi, Surekha Reddy Bandela, Ilhami Colak, J. Nageswara Rao, and A. Rajaram. "Prediction of biomedical signals using deep learning techniques." *Journal of Intelligent & Fuzzy Systems* Preprint (2023): 1-14. https://doi.org/10.3233/JIFS-230399
[14] Tamilarasi, K., K. Maheswari, S. Ramesh, Samson Isaac, and A. Rajaram. "A Decentralized Smart Healthcare Monitoring System using Deep Federated Learning Technique for IoMT." (2023).
[15] Yagoub, Sami Abdelrahman Musa, Gregorius Eldwin Pradipta, and Ebrahim Mohammed Yahya. "Prediction of bubble point pressure for Sudan crude oil using Artificial Neural Network (ANN) technique." *Progress in Energy and Environment* (2021): 31-39.
[16] Karim, Abdul Razif Abdul, and Roslina Mohammad. "Meta-study of sensitivity analysis in solar renewable energy application." *Progress in Energy and Environment* (2023): 14-25. https://doi.org/10.37934/progee.23.1.1425
[17] Chiranjeevi, Phaneendra, and A. Rajaram. "A lightweight deep learning model based recommender system by sentiment analysis." *Journal of Intelligent & Fuzzy Systems* Preprint (2023): 1-14. https://doi.org/10.3233/JIFS-223871
[18] Harikrishnan, G., and A. Rajaram. "Improved throughput based recognition connection denies for aggressive node in wireless sensor network." *Journal of Computational and Theoretical Nanoscience* 14, no. 12 (2017): 5748-5755. https://doi.org/10.1166/jctn.2017.7008
[19] Rosario, B. BERIL DANIEL, and A. Rajaram. "CDMA based secure cross layer framework for authentication and scheduling in MANET." *Journal of Theoretical and Applied Information Technology* 69, no. 3 (2014).
[20] Mukundan, V., A. Rajaram, and S. Gopinath. "Securing Mobile Ad Hoc Network using Double Hash Authentication technique."
[21] Palaniswami, S., and Ayyasamy Rajaram. "An enhanced distributed certificate authority scheme for authentication in mobile ad hoc networks." *The International Arab Journal of Information Technology (IAJIT)* 9, no. 3 (2012): 291-298.
[22] Rajaram, A., and S. Palaniswami. "A high certificate authority scheme for authentication in mobile ad hoc networks." *International Journal of Computer Science Issues (IJCSI)* 7, no. 4 (2010): 37.
[23] Indira, D. N. V. S. L. S., Rajendra Kumar Ganiya, P. Ashok Babu, A. Xavier, L. Kavisankar, S. Hemalatha, V. Senthilkumar *et al.,* "Improved artificial neural network with state order dataset estimation for brain cancer cell diagnosis." *BioMed Research International* 2022 (2022). https://doi.org/10.1155/2022/7799812
[24] Sathiyaraj, K., and A. Rajaram. "An optimized design modelling of neural network based green house management system using solar and rectenna." *DYNA–Ingen. Ind* 97, no. 1 (2022): 85-91. https://doi.org/10.6036/10089

AMERICAN SCIENTIFIC PUBLISHERS

Journal of
Nanoelectronics and Optoelectronics
Vol. 19, pp. 1042–1052, 2024
www.aspbs.com/jno

ARTICLE

Improved Finger Vein Recognition Using Generative Adversarial Network and Transfer Learning

Amitha Mathew* and P. Amudha

The unique and secure nature of Finger Vein Recognition (FVR) has attracted considerable attention in the field of biometric authentication. However, challenges such as limited data availability and the complexity of vein patterns necessitate innovative approaches to improve recognition performance. A novel approach to FVR is proposed using Pix2Pix style Generative Adversarial Networks (GANs) for finger vein dataset augmentation providing synthetic images for training VGG16 model. The main objective of the paper is to enhance the quality and diversity of Finger Vein (FV) datasets while improving the robustness of the recognition system. Our approach involves training a GAN to generate realistic finger vein images that encapsulate the intricate vein patterns present in real-world scenarios. The study evaluates the proposed approach on the THU-FVFDT1 dataset, considering conventional augmentation and GAN-based augmentation. The results demonstrate that transfer learning from a conventionally augmented dataset to one augmented with GANs yields superior performance, as evidenced by the evaluation metrics. The experimental findings illustrate the effectiveness of dataset augmentation and transfer learning in the realm of finger vein recognition for biometric identification.

Keywords: Biometric Systems, Finger Vein Recognition (FVR), Generative Adversarial Networks (GAN), Dataset Augmentation, VGG16.

1. INTRODUCTION

Biometric technology finds applications in various sectors including access control, financial transactions, healthcare, government, technology, education as well as private organizations. The biometrics has significantly contributed to reducing corruption, enhancing the cost-effective delivery of public services, and minimizing intermediaries. Finger Vein Recognition has emerged as a promising biometric authentication method, offering a highly secure and non-intrusive means of verifying individuals' identities. Finger vein biometric relies in the fact that veins absorb infrared light differently than the surrounding tissues, creating a complex and distinct pattern that can be captured using near infrared light to illuminate the finger. The unique nature of vein patterns makes it highly secure, as the likelihood of two individuals having identical finger vein patterns is extremely low [1]. Since the veins are located below the skin, it is less susceptible to spoofing or tampering compared to surface level biometrics like fingerprints. The effectiveness of such systems heavily relies on the excellence of feature extraction and its representation. FVR is a good research area, aiming to exploit the unique and complex patterns of blood vessels beneath the skin's surface for accurate identification.

Traditional methods in finger vein recognition have predominantly relied on handcrafted features and conventional machine learning algorithms like k-nearest neighbours (k-NN) [2–4] and Support Vector Machines [5–7]. While effective to a certain extent, these methods often need help to capture the intricate details of finger vein patterns and might be susceptible to variations in image acquisition conditions. In recent years, researchers have explored deep learning techniques for improved FVR. Convolutional Neural Networks (CNNs) demonstrated encouraging results in automatically learning discriminative features from raw finger vein images [8, 9]. Transfer learning is how pre-trained CNN models are fine-tuned on specific finger vein datasets and has also demonstrated enhanced performance.

Department of Computer Science and Engineering, Avinashilingam Institute for Home Science and Higher Education for Women, Coimbatore 641043, India
*Author to whom correspondence should be addressed.
Email: 18pheop002@avinuty.ac.in
Received: 25 May 2024
Accepted: 26 May 2024

Most of the deep learning algorithms shows poor performance due to the lack of data, with diverse features. Insufficient data can lead to poor model performance. While training a deep learning model with finger vein images most of the database consists of images of different subject with less image per subject. The number of images utilized for training per subject significantly impacts the verification performance of the model. To withstand this disadvantage, two approaches were considered for augmentation. The first involves traditional transformation methods such as rotation, shifting, brightness variations, and zooming. In the second approach, we leveraged Generative Adversarial Networks (GANs) for augmentation, which has proved to be efficient in generating images in various other domains. In recent years, GANs have gained significant attention for their exceptional ability to generate data for dataset augmentation [10–13]. Our approach involves addressing the challenges of data scarcity and varying features in a finger vein image dataset by leveraging GANs to generate synthetic images. These generated images are then combined with the original dataset for training a CNN model, with the overall goal of improving the model's performance in identification and verification tasks.

We have considered the THU-FVFDT1 data which consists of two images taken in two different sessions for a single individual. Hence only one image per individual can be used for training as the other one is reserved for testing. But training a deep model using this single image shows poor performance which is not acceptable for a recognition task in a real-world scenario. In this work GANs are used to augment FV images, aiming to enhance the accuracy and robustness of FVR systems. GANs comprise two parts: generator and discriminator. The generator network is tasked with producing images that are indistinguishable from genuine finger vein samples, while the discriminator network learns to differentiate between real and fake data. This adversarial interplay leads to the creation of highly realistic and authentic images. During training GAN learns the underlying patterns and intricacies of vein structures. As a result, the generator becomes proficient in crafting synthetic vein patterns that are visually convincing and coherent. This process inherently aids in creating comprehensive and diverse representations of finger vein data. By leveraging GANs to generate representative finger vein images, it becomes possible to address data scarcity issues and enhance the generalization capabilities of recognition models. The synthesized images can capture the variability present in real-world scenarios, leading to improved performance under various conditions.

Our work is distinguished by the following key features:
1. The training of GAN for image generation requires meticulous balancing to prevent the discriminator from overpowering the generator. Addressing these challenges is critical to ensure that the generated representations are accurate and effective for authentication purposes.
2. The experimental methodology discusses the dataset, the network architecture of the GAN, and the performance metrics utilized for assessing the quality of the generated FV representations.
3. To evaluate the performance of the augmented dataset, we utilize a VGG16 convolutional network with various training methods, including training with the original dataset, conventional augmented dataset, GAN augmented dataset, and the transfer learning method.

The overall objective is to enhance the dataset using conventional method and GANs, utilizing it for training purposes to improve the effectiveness of biometric systems based on FV recognition. In the subsequent sections of this paper, the associated literature are explored in Section 2, Section 3 details the methodology for augmenting the dataset, evaluation methods and results of augmentation are discussed in Section 4, and Section 5 gives the conclusion and future works.

2. RELATED WORKS

FVR can be deemed more secure than other hand-based biometric characteristics like fingerprints and palm prints, primarily because its distinguishing features are within the human body. Several researches are conducted to explore and advance various methodologies, algorithms, and technologies striving to improve efficiency of FV authentication system.

Rosdi et al. [14] present a finger vein personal verification mechanism in which the local line binary pattern (LLBP), is used as a feature extraction tool. In contrast to the local binary pattern (LBP), where the neighbourhood shape is square, the local shape in LLBP is a straight line. Kumar et al. [15] put forward a method for enhancing finger-vein recognition systems' performance where the system concurrently collects low-resolution finger vein and finger-print images, then combines them using score-level combination method. The low-resolution fingerprint-matching performance of images and their usability are determined. Wu et al. [16] provide an SVM technique for identifying FV patterns. The FV pattern is difficult to see in visible light. Therefore, the device uses an infrared LED and a CCD camera to capture it. The verification system consists of pattern classification and picture preprocessing. The study reduces the dimensionality of the images and retrieves their properties using principal component analysis (PCA) and linear discriminant analysis (LDA). This system combined an SVM and an adaptive neuro-fuzzy inference method to categorise patterns. The significant feature is retained with LDA, while noise is decreased in the disregarded dimensions using the PCA approach. The characteristics are then employed to categorise data and find patterns.

Peng et al. [17] presented a technique that is put forward for biometrically validating infrared finger-vein patterns.

They initially configured a Gabor to utilise the FV network. They obtained vein patterns by combining results from two distinct orientations and incorporated SIFT features to mitigate the influence of image rotation and shifting. The number of features that match the enrolled and test FV patterns is the basis for personal identification verification. Qin et al. [18] describe a novel technique for upgrading FVR systems with a method for extracting finger-vein shape and orientation data using vein pattern extraction. To effectively consider inherent variations, a region-based matching strategy is studied utilising the Scale Invariant Feature Transform (SIFT) approach. The SIFT features, FV shape, and orientation are merged to improve performance even more.

A finger-vein recognition system utilizing CNN that demonstrates resilience to misalignment and shading challenges associated with finger veins was proposed in Ref. [8]. The research also emphasizes the significance of lack of abundant training data for the successful training of the deep CNN model. Shao et al. [19] presented PalmGAN, a method designed to augment a palmprint dataset containing associated labels. The researchers employed an auto-encoder structured model to perform domain adaptation [20]. The increasing global concern over contact-transmitted diseases such as COVID-19 emphasize the need for a more resilient touchless biometric recognition system [21]. The Table I shows more existing works based on the finger vein representation with their advantages and limitations.

Existing works on finger vein recognition have made significant advancements in biometric authentication, but they still face several limitations:

1. The accuracy of recognition can be changed according to variations in finger position, lighting conditions, and the quality of imaging devices, leading to potential false positives or false negatives.
2. Collecting finger vein data can be intrusive and uncomfortable for users, hindering widespread adoption. The need for standardized datasets and evaluation metrics makes comparing different algorithms and systems challenging.
3. The vulnerability of FVR to spoofing attacks, where an attacker uses fake vein patterns, underscores the need for robust anti-spoofing techniques to enhance security.

Overcoming these limitations is crucial for the continued development and deployment of finger vein recognition systems.

3. METHODOLOGY

3.1. Proposed System: Overview

We explored different approaches for evaluating the impact of data augmentation in improving the performance of the classification model using the VGG16. Initially VGG16 is trained using the original dataset without using any augmentation techniques. The performance of this model can be used as a baseline for comparison with augmented datasets. Then dataset1 is created using conventional augmentation methods by applying different transformation operations on the original dataset. The VGG16 model is then trained using dataset1 to observe improvements in performance. Subsequently dataset2 is generated using GAN that mimics the distribution of original dataset and capturing more diverse patterns. The VGG16 model is trained using the dataset2 which includes realistic synthetic samples created by GAN. In the transfer learning approach, the VGG16 model is initially trained on Dataset1, and the pre-trained model undergoes further fine tuning using Dataset2 to leverage knowledge gained from the first training phase. Figure 1 illustrates the conceptual framework of the proposed system.

The study is focused on enhancing the representation and recognition of finger vein patterns and provide a safe

Table I. Prior Studies: Strength and weakness.

Author	Methodology	Advantages	Limitations
Zhange et al. [22]	Lightweight and fully convolutional GAN architecture.	Improved recognition accuracy and enhanced data diversity.	Complexity in GAN training.
Wei-Feng Ou et al. [23]	Employed GANs to synthesize finger vein images. Leveraged generator-discriminator interplay for realistic data creation.	Expanded dataset for training and reduced overfitting.	Balance between real and synthetic data. Possible mode collapse in GAN.
Jiho Choi et al. [24]	Modified conditional GAN and CNN	Improved feature learning	Complexity in GAN-based feature extraction
Qiong Yao et al. [25]	Siamese network framework (Siamese Gabor residual network)	Robustness against limited data	Dependency on adequate positive pairs
Jalilian et al. [26]	Fully Convolutional Network (FCN)	Enhanced generalization.	Unsatisfactory when tested in a cross-domain setting.
Dabouei et al. [27]	Conditional Generative Adversarial network (CGAN)	Evaluated the effectiveness in a cross-sensor environment.	Limited to available vein patterns.
Nogueira et al. [28]	Visual Geometry Group16 (VGG16)	Robustness to variations.	Ineffective when applied in a cross-data, cross-sensor environment

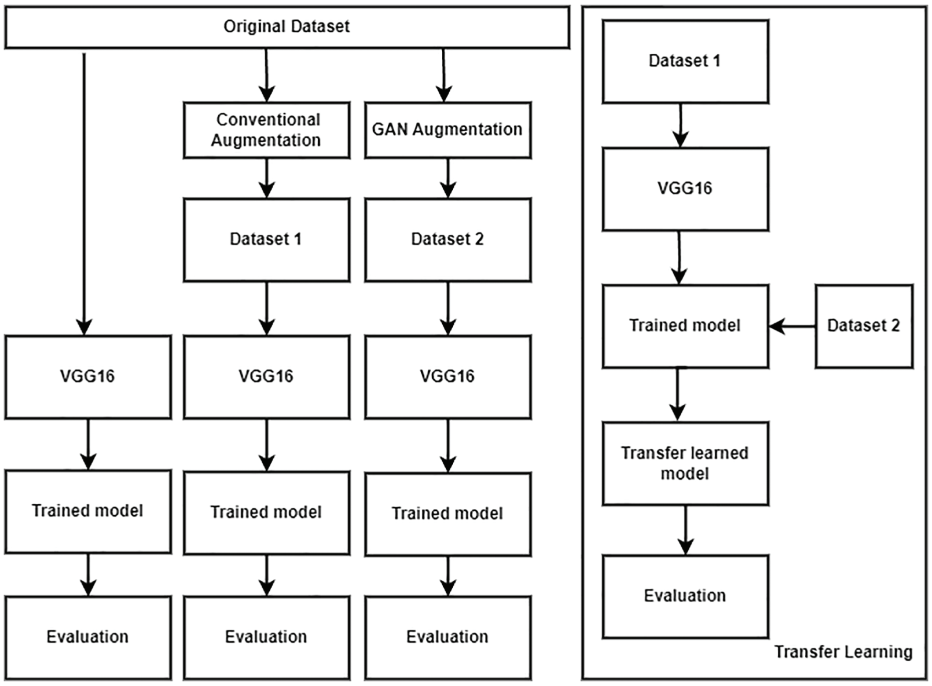

Fig. 1. Proposed system: Overview.

method of biometric identification, by utilizing the capabilities of GANs for augmenting the dataset.

3.2. Dataset and Experiment Environments

The original data used in our research is from THU-FVFDT1 [29] which contains 220 different subjects' raw FV images. The images are obtained from Tsinghua University Graduate School students and staff. Raw images have a resolution of 720×576 pixels. Two images per subject captured in two sessions are available in this dataset. We used THU-FVFDT1 in our experiments because it includes images of nonuniform illumination and has been widely used in previous research on FV recognition.

The computational for this study used a PC with an Intel I5-8300H CPU-2.30 GHz, 16 GB of RAM, NVIDIA GTX 1050 graphic processing unit card and 8 GB of graphics memory. TensorFlow 2.8, Keras 2.7 and other necessary libraries were used to implement the algorithms and models.

3.3. Preprocessing

The images from the dataset are pre-processed. The backdrop is eliminated during preprocessing to identify the finger region of interest. The mean pixel value along the x-axis is used to determine the finger's left and right endpoints. This is achieved by summing all the pixel values along the y-axis relative to the x-axis. When the computed average pixel value equals or surpasses a predefined threshold, the two boundary lines of the finger region are established based on these values. The finger area's upper and lower boundary lines are then identified through a 4×20 mask applied as a filter operation. If the boundary lines are incorrectly identified, a corrective method is employed. A comparison is made between the y-axis boundary line coordinates and the average value of the x-axis boundary line coordinates. When a significant discrepancy exists between the detected value and the mean value, the points are then eliminated. The remaining points are utilized update the boundary line. Finally, bilinear interpolation is utilized to resize the determined finger Region of Interest (ROI) to 256×256 [30].

3.4. Dataset Augmentation

We have used two methods of augmentation. The first one is augmentation using conventional transformation methods and the second one uses a Pix2Pix GAN for image augmentation which are explained in the following sections.

3.4.1. Conventional Augmentation

A combination of Local Maximum Curvature (LMC) algorithm, Repeated Line Tracking (RLT) algorithm, and Wide Line Detector (WLD) algorithm is utilized for extract baseline finger vein patterns and the resulting images are combined to get optimal vein pattern [31]. The merged image is augmented using traditional transformation methods such as rotation, shifting, brightness variations and zooming. The utilization of baseline extracted finger vein images accelerates the training of deep learning algorithms, thereby reducing the overall training duration. Ten image per individual is created using transformation from the original image.

3.4.2. Augmentation Using GAN

GAN comprises a discriminator model that can tell the difference between actual and fake images produced by the generator model. Both models are trained to compete against one another while maintaining an adversarial relationship. So, they may create an unreal image that looks real. The typical GAN design is depicted in Figure 2 [28].

The manually labelled vein images are provided as additional information, which allows to condition the image generation process on specific class. This additional information helps to maintain specific vein patterns in the augmented images. Thus, this helps to generate variations of labelled images for expanding dataset by keeping the semantic meaning intact. This work employs the Pix2Pix style GAN for image augmentation. Pix2Pix GAN is a type of conditional GAN (cGAN) which utilizes additional information to condition the generator and discriminator to create correct images of finger veins that reflect the variety and complexity of actual finger vein patterns. The generator's output is improved over iterative training by the discriminator, which is skilled at identifying actual images from produced ones [32]. The generated finger vein images are subsequently assessed using VGG16 for finger vein recognition.

The images in the dataset are manually labelled. These manual labels are used as ground truth images for conditioning the GAN. Figure 3 shows sample original images from the dataset and the corresponding manually labelled images.

The Pix2Pix style GAN, which generates an image from another image is shown in Figure 4. Here, we are training two models against each other in which one is the generator, and the other is the discriminator. The generator model generates fake images using an autoencoder; the activation function is tanh which is calculated using the Eq. (1). The tanh has an output ranging from -1 to 1, which squashes the output to a specific range making it easier to learn and reconstruct the input data. Since it is zero centered, it helps to mitigate vanishing gradient problem and thus aids in better convergence of the model.

$$f(x) = \frac{e^x - e{-}^x}{e^x + e{-}^x} \tag{1}$$

The discriminator is a standard model with the leaky ReLU and sigmoid activation function. The leaky ReLU activation is calculated using the Eq. (2),

$$f(x) = \max\ (0.01 * x,\ x) \tag{2}$$

This function returns x for a positive value and small value for a negative number which ensures the network can still learn from negative inputs.

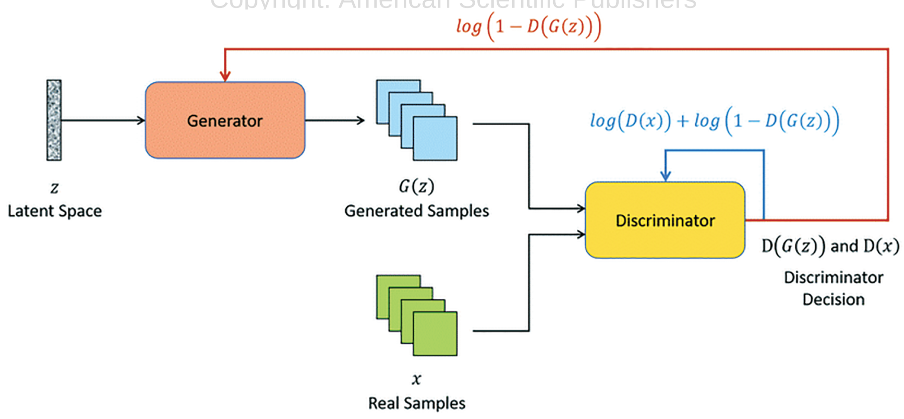

Fig. 2. Typical GAN architecture.

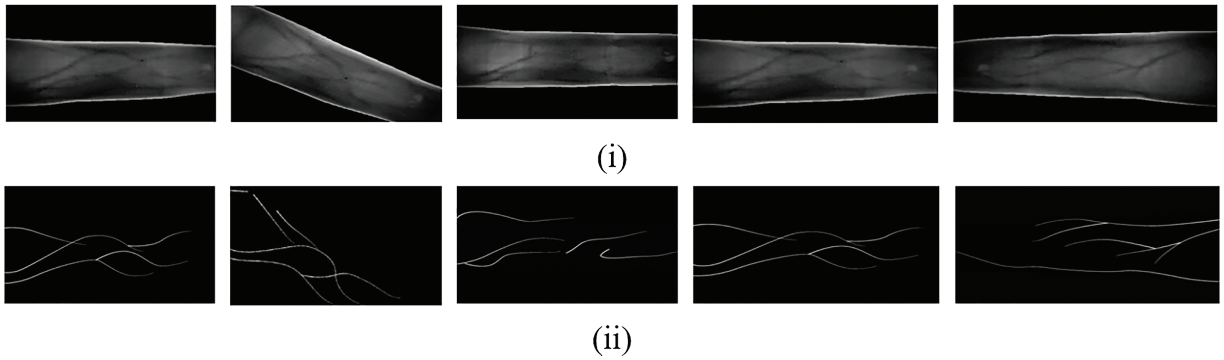

Fig. 3. (i) Original image (ii) manually labelled image.

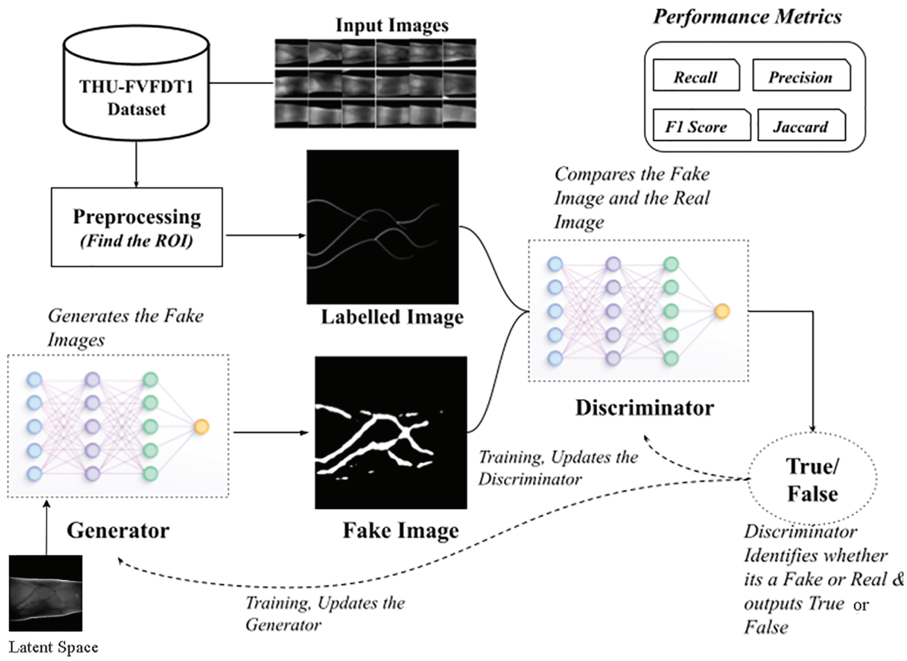

Fig. 4. GAN for finger vein image augmentation.

The discriminator's role is a binary classification of realistic and fake finger vein images. The sigmoid activation function shown in Eq. (3), squashes the discriminator output to the range [0, 1]. The output can be interpreted as real if closer to 1 and fake if closer to 0.

$$f(x) = \frac{1}{1+e-^{x}} \tag{3}$$

The discriminator model has two inputs: one is the labelled image, and the other is a fake image generated by the generator; then, it checks whether the fake image matches with the required output or not and returns true or false as the output. The generator model has been trained to create the best fake image so that the decrease in loss of the model will show how efficient the generator is. These models are trained one at a time. The generator will be trained first, and the output will be stored. Then, the discriminator is trained, compares the actual output with the fake image, and checks the loss value. Then again, the generator is trained to improve its performance and goes in a loop. Finally, the model performance is evaluated. Through adversarial training, the GAN learns the intricate mapping between source images and the corresponding target images.

The training process of GAN involves training one model at a time. The generator is fixed when training the discriminator. The discriminator is updated using the Eq. (4),

$$\nabla_{\theta_d} \frac{1}{m} \sum_{i=1}^{m} \left[\log D\left(x^{(i)}\right) + \log\left(1 - D\left(G\left(z^{(i)}\right)\right)\right)\right] \tag{4}$$

Where "x" is the real data, "z" is the latent vector, "$G(z)$" is fake data, "$D(x)$" signifies the discriminator's evaluation of real data, "$D(G(z))$" also represents the

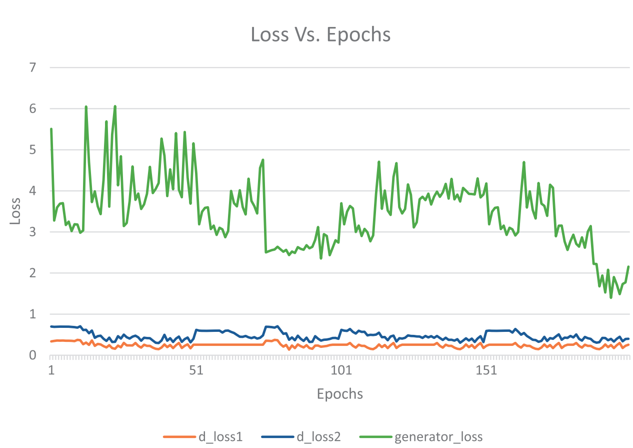

Fig. 5. Generator and discriminator loss for 200 epochs.

Table II. Loss values for different epochs.

Epochs	d_loss1	d_loss2	Generator loss
1	0.3360	0.3610	4.8100
25	0.1930	0.2130	4.4360
50	0.2560	0.1450	4.7540
75	0.3530	0.3410	1.8093
100	0.2560	0.1450	2.3400
125	0.2560	0.2130	3.4360
150	0.1750	0.1450	3.5900
175	0.2450	0.2130	2.4360
200	0.2560	0.1450	1.7540

discriminator's evaluation of fake data. The generator is updated using Eq. (5), which is calculated as,

$$\nabla_{\theta_d} \frac{1}{m} \sum_{i=1}^{m} \log\left(1 - D\left(G\left(z^{(i)}\right)\right)\right) \tag{5}$$

In this, z represents the Latent vector. The generator and discriminator are two separate models that interact to form the GAN, and each model will have a unique loss function. The discriminator's loss function is represented using Eq. (6):

$$LD = Loss\left(D\left(x\right), 1\right) + Loss\left(D\left(G\left(z\right)\right), 0\right) \tag{6}$$

The generator is also treated in the same way. The discriminator must be as perplexed as possible for the generator to succeed in mislabelling produced images as real. The generator loss is represented in the Eq. (7).

$$LG = Loss\left(D\left(G\left(z\right)\right), 1\right) \tag{7}$$

The loss values represent key indicators of the training progress and performance of the GAN. They are integral for evaluating the GAN's ability to generate realistic finger vein images from source images effectively. So here we are considering three loss values which are explained below.

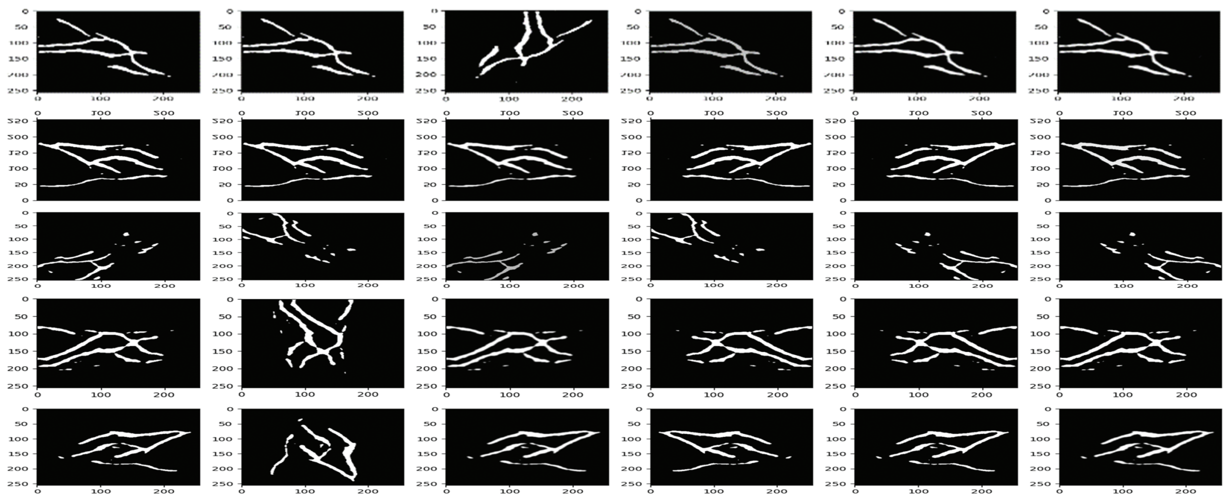

Fig. 6. Augmented images using conventional transformations.

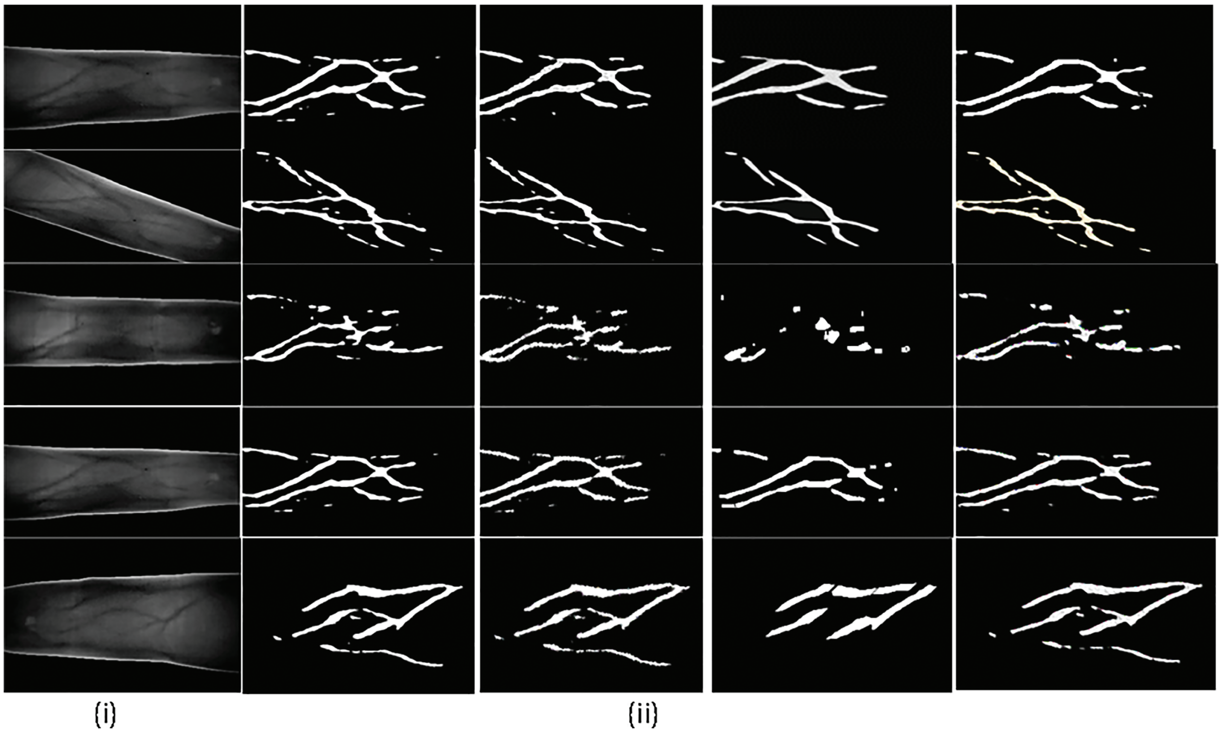

Fig. 7. GAN generated images: (i) Input image (ii) sample GAN generated images.

d_loss1 (Discriminator Loss on Real Images): This loss quantifies how well the Discriminator distinguishes real images (ground truth) from fake ones. A lower value indicates improved real image classification.

d_loss2 (Discriminator Loss on Fake Images): This loss measures how effectively the Discriminator recognizes generated (fake) images as distinct from real ones. A lower value signifies better fake image classification.

generator_loss (Generator Loss): This combined loss assesses the performance of the generator network in producing convincing FV images. It consists of adversarial loss, encouraging realistic images, and $L1$ loss, promoting similarity to target images.

The d_loss1, d_loss2 and generator_loss at different epochs of trainings are shown in Table II. The loss values seem to fluctuate which is common in GAN training as the generator and discriminator is in a constantly competing. The low discriminator values indicate the discriminator is having difficulty in distinguishing real and generated samples which means the generator is performing well in generating realistic samples. The lower loss values of generator also indicate better performance. The graph depicting the d_loss1, d_loss2 and generator loss for 200 epochs are shown in Figure 5.

4. EVALUATION OF THE AUGMENTED DATASETS

We are considering two methods to evaluate the quality and diversity of the augmented datasets which are described in the following sections.

4.1. Visual Inspection

The sample augmented images using conventional transformations are shown in Figure 6. The images appear in different orientations and lighting scenario. The systematic rotation helped in creating images from various angles, shifting introduces spatial variability, simulating changes in finger placement, brightness variations reflect adaptability to different lightning conditions. The visual observation of the created images underscores the success of transformations in creating more comprehensive dataset.

A set of sample images generated by the Pix2Pix GAN are showcased in Figure 7. These images are the result of the GAN's ability to autonomously produce synthetic finger vein images based on the patterns it has learned during the training process. Each image in Figure 6 is a visual representation of the network's creative output, reflecting its capacity to generate diverse and realistic variations of finger vein patterns.

Upon closer inspection of the displayed images, one can discern noticeable variations and nuances within the generated dataset. Through visual observation, we gain insights into the GAN's proficiency in introducing subtle changes, creating a spectrum of unique finger vein patterns. This demonstrates the GAN's effectiveness in not only mimicking the input data but also in producing a diverse array of synthetic images contributing to the augmentation of the original dataset and subsequently enhancing the robustness of the finger vein recognition.

The successful deployment of a Pix2Pix-style GAN architecture has showcased its adaptability to the domain

Table III. Details of dataset for various approaches.

	Original	Conventional augmentation	GAN augmentation	Transfer learning
No: of images per individual	1	10	30	40
Total images	220	2200	6600	8800

Table IV. Performance metrics calculation.

Performance metric	Equation
Accuracy	$\dfrac{TP+TN}{TP+FP+TN+FN}$
F1 score	$2\times\left(\dfrac{TP}{TP+FP+FN}\right)$
Recall	$\dfrac{TP}{FN+TP}$
Precision	$\dfrac{TP}{TP+FP}$

Table V. Performance of various approaches.

Approach	Accuracy	Recall	Precision	F1 score
VGG16	0.925	0.9409	0.9764	0.9583
VGG16 + Conventional augmentation	0.953	0.9693	0.977	0.9731
VGG16 + GAN augmentation	0.974	0.9875	0.983	0.9852
Transfer learning	0.9867	0.9886	0.9961	0.9923

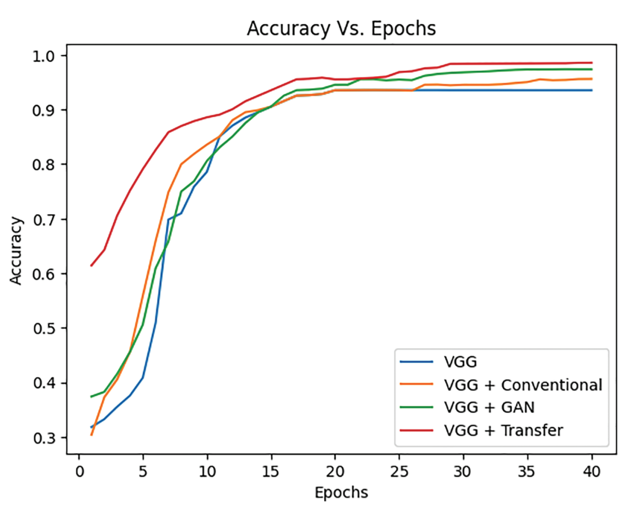

Fig. 8. Accuracy plot for various approaches.

Table VI. Comparison with other methods.

Method	Traditional machine learning				Deep learning					
	CFFR [33]	KNN [34]	kNCN [35]	SVM [36]	AlexNet [37]	Patch-DNN + P-SVM [38]	DNN + P-SVM [39]	VGG19 [37]	CNN [40]	Proposed method
Accuracy	22.3%	69.7%	78.64%	71%	70.2%	79.9%	81.98%	87.57%	95.13%	98.67%

of FVR, enabling the translation of source finger vein images into highly authentic representations. By harnessing adversarial training and the interplay between generator and discriminator networks, the GAN has learned to produce images that align with the unique characteristics of FV patterns.

4.2. Evaluation of Recognition Performance Using VGG16

To assess the effectiveness of our GAN-augmented dataset in enhancing the recognition of the individuals, we used a VGG16 architecture, known for its robust performance. Initially, we trained the VGG16 model on the original dataset, featuring one image per individual across 220 subjects. Subsequently, we conducted training and evaluation using a dataset augmented through conventional transformation methods, incorporating ten images per individual. Following this, the GAN-augmented dataset, comprising 30 images per individual, was utilized for training. Additionally, we employed a transfer learning by retraining the model initially trained on the conventional augmented dataset with the GAN-augmented dataset. The details of the datasets used for different training strategies are shown in Table III.

The effectiveness of various methods' is evaluated by calculating the following metrics as detailed in Table IV.

- *F1 Score:* It reflects the harmonic mean of the recall and precision, capturing the trade-off between the two.
- *Recall*: This metric calculates the proportion of actual positive cases correctly identified by the model.
- *Precision*: it signifies the fraction of positive predictions that are truly positive.

Here, TP = True Positive, FP = False Positive, TN = True Negative, FN = False Negative. The performance metrics for the various approaches considered are shown in Table V. Conventional and GAN augmentation techniques shows better the performance, compared with the model trained using original dataset. Transfer learning leveraging knowledge gained from conventional augmented dataset and retained on GAN augmented dataset shows highest performance across all metrics. The high precision and recall values indicate a well-balanced model capable of accurate individual recognition.

The combined accuracy graph for various approches are plotted in Figure 8. The graph clearly indicates that both augmentation strategies contribute towards increasing accuracy, amongst GAN augmentation shows better performance. Transfer learning excels over the other approaches, owing to it's utilization of pretrained knowledge.

Our proposed model is compared with the existing methods in Table VI. Deep learning methods shows higher accuracy than traditional machine learning methods. Among the deep learning approaches the proposed model, combining dataset augmentation and transfer learning approach outperforms both traditional and deep learning methods.

Using GANs for finger vein augmentation is considered advantageous compared to other models. GANs offer a powerful framework for generating realistic finger vein patterns, making them a strong choice for augmenting dataset especially for biometric authentication task when only few images are available for training the deep models. The adversarial training process enables GANs to capture intricate vein patterns, improve recognition accuracy, and enhance security against spoofing attacks, ultimately making them a promising and effective approach for FV recognition.

5. CONCLUSION

In this work, we systematically assessed the effectiveness of different data augmentation approaches for finger vein pattern recognition in biometric identification using VGG16 architecture. The study was conducted using the THU-FVFDT1 dataset. Initial training on the original dataset without augmentation served as a baseline. Dataset1 created using Conventional augmentation and Dataset2 generated using GAN augmentation demonstrated improved model performance, with GAN augmentation showing particularly promising results. The visual inspection of results, showcasing source images and generated images side by side, has underscored the GAN's proficiency in capturing the intricate vein patterns present in finger vein images. The transfer learning approach, where the model was initially trained on Dataset1 and fine-tuned on Dataset2, yielded the highest recognition accuracy of 98.67%. Precision, recall, and F1 score measurements also indicate that the model is well-balanced and is capable of accurate individual identification. The comparison with existing models highlighted the superiority of our proposed model, combining dataset augmentation and transfer learning, over traditional machine learning approach. Our proposed model consistently outperformed other deep learning approaches also, emphasizing the effectiveness of augmenting datasets and leveraging transfer learning for finger vein pattern recognition in biometric identification. Although the methodology and experimental findings showcased notable achievements, there are still opportunities for additional exploration and fine-tuning. Enhancements to the VGG16 architecture could potentially achieve higher recognition performance. Additionally, the dataset augmentation strategy deserves investigation with diverse datasets, varying in quality, to comprehensively assess its effectiveness and generalizability.

DECLARATIONS

Ethics Approval and Consent to Participate

This article does not contain any studies with human participants or animals performed by any of the authors.

Consent for Publication

All contributors agreed and given consent to Publication.

Availability of Data and Material

Data that has been used is confidential.

Competing Interests

On behalf of all authors, the corresponding author states that they have no competing interest.

Authors' Contributions

The authors confirm contribution to the paper as follows and all authors reviewed the results and approved the final version of the manuscript. Amitha Mathew Writing original draft, Methodology, study conception and design, Reviewing and editing, analysis and interpretation of results. P. Amudha Data collection, Reviewing and editing Conceptualization.

References and Notes

1. Ye, Y., Zheng, H., Ni, L., Liu, S. and Li, W., **2016**. A Study on the Individuality of Finger Vein Based on Statistical Analysis. *In 2016 International Conference on Biometrics (ICB)*, pp.1–5.
2. Rosdi, B.A., **2016**. Finger vein identification based on the fusion of nearest neighbour and sparse representation-based classifiers. *Indian Journal of Science and Technology 9*(48), pp. 1–7.
3. Mobarakeh, A.K., Rizi, S.M., Khaniabadi, S.M., Bagheri, M.A. and Nazari, S., **2012**. Applying weighted K-nearest centroid neighbour as classifier to improve the finger vein recognition performance. *In 2012 IEEE International Conference on Control System, Computing and Engineering*, pp.56–59.
4. Shazeeda, S. and Rosdi, B.A., **2019**. Finger vein recognition using mutual sparse representation classification. *IET Biometrics*, *8*(1), pp.49–58.
5. Park, K.R., **2011**. Finger vein recognition by combining global and local features based on SVM. *Computing and Informatics*, *30*(2), pp.295–309.
6. Lee, H.C., Kang, B.J., Lee, E.C. and Park, K.R., **2010**. Finger vein recognition using weighted local binary pattern code based on a support vector machine. *Journal of Zhejiang University SCIENCE C*, *11*(7), pp.514–524.
7. Kapoor, K., Rani, S., Kumar, M., Chopra, V. and Brar G. Singh Brar, **2021**. Hybrid local phase quantization and grey wolf optimization based SVM for finger vein recognition. *Multimedia Tools and Applications*, *80*, pp.15233–15271.
8. Hong, H.G., Lee, M.B. and Park, K.R., **2017**. Convolutional neural network-based finger-vein recognition using NIR image sensors. *Sensors*, *17*(6), p.1297.
9. Xie, C. and Kumar, A., **2019**. Finger vein identification using convolutional neural network and supervised discrete hashing. *Pattern Recognition Letters*, *119*, pp.148–156.
10. Frid-Adar, M., Diamant, I., Klang, E., Amitai, M., Goldberger, J. and Greenspan, H., **2018**. GAN-based synthetic medical image augmentation for increased CNN performance in liver lesion classification. *Neurocomputing*, *321*, pp.321–331.
11. Bowles, C., Chen, L., Guerrero, R., Bentley, P., Gunn, R., Hammers, A. and Rueckert, D., **2018**. Gan augmentation: Augmenting training data using generative adversarial networks. arXiv preprint arXiv:1810.10863.
12. Antoniou, A., Storkey, A. and Edwards, H., **2017**. Data augmentation generative adversarial networks. arXiv preprint arXiv:1711.04340.
13. Zhang, J., Lu, Z., Li, M. and Wu, H., **2019**. GAN-based image augmentation for finger-vein biometric recognition. *IEEE Access*, *7*, pp.183118–183132.
14. Rosdi, B.A., Shing, C.W. and Suandi, S.A., **2011**. Finger vein recognition using local line binary pattern. *Sensors*, *11*(12), pp.11357–11371.
15. Kumar, A. and Zhou, Y., **2011**. Human identification using finger images. *IEEE Transactions on Image Processing*, *21*(4), pp.2228–2244.
16. Wu, J.D. and Liu, C.T., **2011**. Finger-vein pattern identification using SVM and neural network technique. *Expert Systems with Applications*, *38*(11), pp.14284–14289.
17. Peng, J., Wang, N., Abd El-Latif, A.A., Li, Q. and Niu, X., **2012**. Finger-vein verification using gabor filter and SIFT feature matching. *In 2012 Eighth International Conference on Intelligent Information Hiding and Multimedia Signal Processing*, pp.45–48.
18. Qin, H., Qin, L., Xue, L., He, X., Yu, C. and Liang, X., **2013**. Finger-vein verification based on multi-features fusion. *Sensors*, *13*(11), pp.15048–15067.
19. Shao, H., Zhong, D. and Li, Y., **2019**. PalmGAN for cross-domain palmprint recognition. *In Proceedings of the 2019 IEEE International Conference on Multimedia and Expo*, Shanghai, China, 8–12, pp.1390–1395.
20. Shao, H., Zhong, D. and Du, X., **2019**. Cross-domain palmprint recognition based on transfer convolutional autoencoder. *In Proceedings of the 2019 IEEE International Conference on Image Processing*, Taipei, Taiwan, 22–25, pp.1153–1157.
21. Malhotra, A., Sankaran, A., Vatsa, M. and Singh, R., **2020**. On matching finger-selfies using deep scattering networks. *IEEE transactions on biometrics. Behaviour, and Identity Science*, *2*(4), pp.350–362.
22. Tran, N.T., Tran, V.H., Nguyen, N.B., Nguyen, T.K. and Cheung, N.M., **2021**. On data augmentation for GAN training. *IEEE Transactions on Image Processing*, *30*, pp.1882–1897.
23. Ou, W.F., Po, L.M., Zhou, C., Rehman, Y.A.U., Xian, P.F. and Zhang, Y.J., **2021**. Fusion loss and inter-class data augmentation for deep finger vein feature learning. *Expert Systems with Applications*, *171*, p.114584.
24. Choi, J., Noh, K.J., Cho, S.W., Nam, S.H., Owais, M. and Park, K.R., **2020**. Modified conditional generative adversarial network-based optical blur restoration for finger-vein recognition. *IEEE Access*, *8*, pp.16281–16301.

25. Yao, Q., Chen, C., Song, D., Xu, X. and Li, W., **2023**. A novel finger vein verification framework based on siamese network and gabor residual block. *Mathematics*, *11*(14), p.3190.

26. Jalilian, E. and Uhl, A., **2018**. Finger-vein recognition using deep fully convolutional neural semantic segmentation networks: The impact of training data. *In 2018 IEEE International Workshop on Information Forensics and Security (WIFS)*, IEEE, pp.1–8.

27. Dabouei, A., Kazemi, H., Iranmanesh, S.M., Dawson, J. and Nasrabadi, N.M., **2018**. ID preserving generative adversarial network for partial latent fingerprint reconstruction. *In 2018 IEEE 9th International Conference on Biometrics Theory, Applications and Systems (BTAS)*. pp.1–10.

28. Nogueira, R.F., de Alencar Lotufo, R. and Machado, R.C., **2016**. Fingerprint liveness detection using convolutional neural networks. *IEEE Transactions on Information Forensics and Security*, *11*(6), pp.1206–1213.

29. Yang, W., Qin, C. and Liao, Q., **2014**. A database with ROI extraction for studying fusion of finger vein and finger dorsal texture. *Biometric Recognition: 9th Chinese Conference, CCBR 2014*, Springer International Publishing, Shenyang, China, Proceedings, Vol. 9, pp. 266–270.

30. Kim, S.G., Choi, J., Hong, J.S. and Park, K.R., **2022**. Spoof detection based on score fusion using ensemble networks robust against adversarial attacks of fake finger-vein images. *Journal of King Saud University-Computer and Information Sciences*, *34*(10), pp.9343–9362.

31. Mathew, A., Amudha, P. and Sivakumari, S., **2023**. Finger vein image labelling using hybrid algorithm. *In Proceedings of the International Conference on Emerging Trends in Industry 4.0 and Sustainable Concepts*. p.978-93-5782-946-5.

32. Aljohani, A. and Alharbe, N., **2022**. Generating synthetic images for healthcare with novel deep pix2pix gan. *Electronics*, *11*(21), p.3470.

33. Shazeeda, S. and Rosdi, B.A., **2018**. Nearest centroid neighbor based sparse representation classification for finger vein recognition. *IEEE Access*, *7*, pp.5874–5885.

34. Damavandinejadmonfared, S., Mobarakeh, A.K., Suandi, S.A. and Rosdi, B.A., **2012**. Evaluate and determine the most appropriate method to identify finger vein. *Procedia Engineering*, *41*, pp.516–521.

35. Rosdi, B.A., Jaafar, H. and Ramli, D.A., **2015**. Finger vein identification using fuzzy-based k-nearest centroid neighbour classifier. *AIP Conference Proceedings*, American Institute of Physics, Washington DC, Vol. 1643, No. 1, pp. 649–654.

36. Wu, J.D. and Liu, C.T., **2011**. Finger-vein pattern identification using SVM and neural network technique. *Expert Systems with Applications*, *38*(11), pp. 14284–14289.

37. Wang, Y., Shi, D. and Zhou, W., **2022**. Convolutional neural network approach based on multimodal biometric system with fusion of face and finger vein features. *Sensors*, *22*(16), p.6039.

38. Qin, H. and El-Yacoubi, M.A., **2017**. Deep representation for finger-vein image-quality assessment. *IEEE Transactions on Circuits and Systems for Video Technology*, *28*(8), pp.1677–1693.

39. Qin, H. and El-Yacoubi, M.A., **2015**. Finger-vein quality assessment by representation learning from binary images. *In Neural Information Processing: 22nd International Conference,* ICONIP 2015, Istanbul, Turkey, November 9-12, 2015, Proceedings, Part I 22, pp.421–431.

40. Qin, H. and El-Yacoubi, M.A., **2017**. Deep representation-based feature extraction and recovering for finger-vein verification. *IEEE Transactions on Information Forensics and Security*, *12*(8), pp.1816–1829.

International Journal of
INTELLIGENT SYSTEMS AND APPLICATIONS IN ENGINEERING
ISSN:2147-6799 www.ijisae.org Original Research Paper

Motion Tolerant Finger Vein Authentication using Deep Learning Techniques

Amitha Mathew[1]*, P. Amudha[2]

Submitted:10/03/2024 **Revised**: 25/04/2024 **Accepted**: 02/05/2024

Abstract: Finger vein authentication offers enhanced security due to the unique and internal nature of vein patterns. However, real-world applications encounter significant issues from motion artifacts and varying image capture conditions, impacting performance and reliability. This study addresses these challenges by utilizing image labelling, dataset augmentation, and a motion-tolerant deep learning architecture. Pixel-wise labelling of finger vein images enhances the model's sensitivity to vein patterns, facilitating data augmentation at the pixel level and improving robustness to environmental variations. The data is enhanced using extensive data augmentation techniques. The proposed methodology combines "Convolutional Neural Networks (CNN)" and "Long Short-Term Memory (LSTM)" for feature extraction and handling motion artifacts. CNN effectively captures spatial features while the LSTM processes temporal information, making the model more resilient to motion artifacts. The model is designed to adapt to different lighting conditions and handle variations in finger positioning, ensuring accurate recognition. This comprehensive approach significantly improves the reliability and performance of finger vein authentication systems in diverse real-world environments.

Keywords: *Dataset Augmentation, Finger Vein Authentication, Finger Vein Image Labelling, LSTM, VGG16*

1. Introduction

Biometric authentication is a critical field focused on ensuring robust security and precise identity verification systems. Traditional methods like fingerprint, facial recognition, and iris scanning are widely adopted but encounter issues such as susceptibility to spoofing, sensitivity to environmental conditions, and variability in user cooperation. In contrast, finger vein authentication has emerged as a promising alternative within biometrics due to the unique and internal nature of vein patterns, which are inherently resistant to forgery and alteration. However, implementing finger vein authentication in real-world scenarios presents challenges, particularly concerning motion artifacts and variations in image capture conditions, which can compromise system performance and reliability. To mitigate these challenges, this study investigates the application of image labelling, dataset augmentation techniques, and the development of a motion-tolerant deep learning architecture. Using these approaches, finger vein authentication can be made more robust and accurate, thereby improving their effectiveness in diverse and dynamic operational environments. [1-3].

The proposed methodology uses the VGG16 architecture, a well-established CNN model, for feature extraction [4]. LSTM networks, known for their capability in handling sequential data and learning temporal dependencies, are incorporated to mitigate the impact of motion artifacts [5-7].

Finger vein image labelling involves identifying and marking specific patterns within the images that correspond to the vein structure. During the labelling process, each pixel is categorized as either vein or background. This detailed labelling allows the deep learning model to capture the intricate complexities of finger vein patterns. It enhances the model's sensitivity to subtle changes in vein patterns, which is critical for applications requiring high accuracy, such as biometric authentication. In pixelwise labelling, the model learns features that are unique to the vein and background regions, improving robustness to variations in lighting, pose, and other environmental factors. It facilitates the application of data augmentation techniques at the pixel level. Augmenting labelled images with variations in pixel values (e.g., brightness, contrast, or rotation) helps models generalize better to data that is unknown. Labelled images reduce ambiguity during training, leading to faster convergence and enhanced model performance [8-9].

To address the limited availability of finger vein images per individual, extensive data augmentation techniques are applied. We have used conventional transformations and deep learning-based augmentation techniques to enhance the existing dataset [10-14].

The proposed model is designed to adapt to different lighting conditions and other environmental factors that affect the quality of the vein images. It also handles variations in the movement or positioning of the user's finger during the scanning process, ensuring accurate recognition even if the finger is not perfectly still [15]. VGG16 is used to extract features, followed by Time Distributed, LSTM, and a dense layer.

The paper is further structured as follows. The research emphasizing the need for image labelling, augmentation, and motion-tolerant deep learning models for precise recognition is reviewed in section 2. The proposed model is discussed in Section 3 followed by the results obtained from various configurations in section 4. Section 5 gives the conclusion.

[1] Research Scholar, Department of Computer Science and Engineering, School of Engineering, Avinashilingam Institute for Home Science and Higher Education for Women, Coimbatore, India – 641108, ORCID: 0000-0003-2802-1738
[2] Professor, Department of Computer Science and Engineering, School of Engineering, Avinashilingam Institute for Home Science and Higher Education for Women, Coimbatore, India – 641108, ORCID: 0000-0001-7763-8633

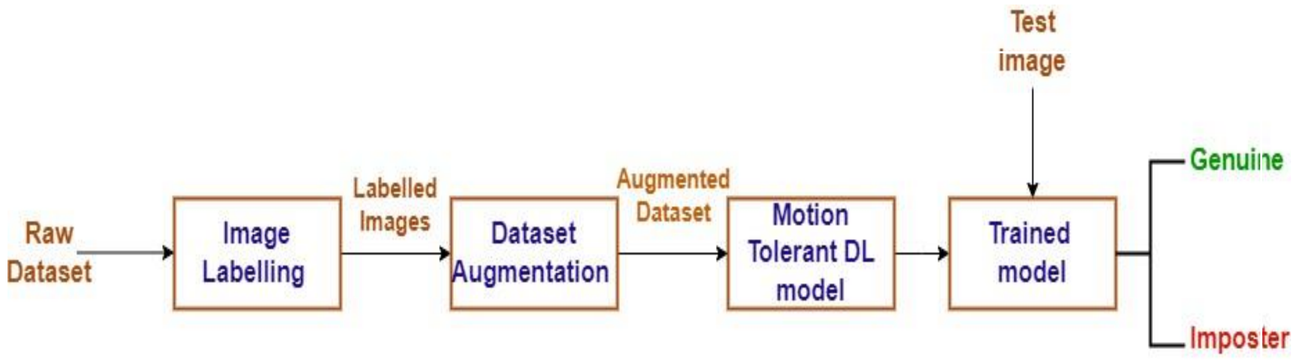

Fig 1. Overview of the motion tolerant finger vein recognition model

2. Related Work

The authors of [16] investigated the use of CNNs for feature learning in finger vein authentication, highlighting that while CNNs are effective, they require substantial computational resources and sufficient training data, posing challenges in their practical application.

The research conducted in [17] using CNN with a stochastic diagonal Levenberg- Marquardt algorithm found that CNNs robustness to noise and misalignments in the acquired images, which enhances their effectiveness for biometric identification. In [18] CNNs are used for labelling and training while the missing vein patterns are recovered using a Fully Convolutional Network (FCN). However, their approach struggled with imbalanced local illumination, presenting a significant challenge for accurate finger-vein verification.

The finger-vein recognition using CNNs with data augmentation was explored in [19], specifically using translation techniques for augmentation. They found that relying solely on translation for augmentation was insufficient, indicating the need for more diverse augmentation strategies to improve recognition performance.

In a study involving deep fully convolutional neural semantic segmentation networks for finger vein recognition, automatic labels significantly increased the network's recognition accuracy, demonstrating the importance of quality training data for model performance [20].

A two-stream convolutional network learning proposed in [21] identified that the limited number of training samples hindered effective training for learning invariant features. Additionally, they noted that preprocessing steps failed to adequately address the change in angles and positioning of fingers, further complicating the training process.

Multimodal biometric recognition by fusing finger-vein and finger-shape data, based on a deep CNN was examined in [22]. They found that most false rejection cases were due to improper alignment of finger-vein images, caused by position changes of fingers during enrollment and recognition phases, highlighting a critical issue in practical biometric systems.

The research in [23] demonstrated that GAN-generated synthetic images can significantly improve the classification accuracy of CNNs by providing additional training examples that capture the variability of real medical images. The authors found that the augmented dataset improved the network's generalization ability, leading to better performance on unseen data than traditional augmentation techniques. The study findings in [24] underscore the potential of GANs to address data scarcity issues which contribute towards improving the robustness and performance of deep models in diverse applications.

The researchers in [25] introduced a method for real time verification of finger-vein biometrics using CNNs and LSTM networks. Their study demonstrated that this approach effectively handles variations in finger movement or positioning during scanning, thereby developing an accurate and robust system.

3. Proposed Method

After extracting the region of interest from the raw dataset, a hybrid algorithm is used to label the dataset. The labelled images are then used to augment the dataset. Conventional transformations and GAN based augmentation are used to expand the database. Deep learning models become more robust and generalizable with augmentation by providing it with a more diverse set of training examples. Using the augmented dataset, a motion-tolerant deep learning model is trained. This model is designed to handle variations and inconsistencies in the input images that might arise from motion, ensuring reliable performance even when the fingers are not perfectly still. A new image, which is not used for training or augmentation, is provided to the trained model for evaluation. The model then can be used to authenticate or reject a person. classifies it as genuine, authentic person or imposter.

3.1 Dataset

The experimentation is conducted with two datasets and the details are given in Table 1. The first dataset is sourced from the "SDUMLA-HMT" database, compiled by Shandong University. A total of 3816 images were scanned from 106 persons. Images of three fingers from both the hands, excluding thump and small finger were captured six times. These images are sized at 320x240 pixels [26]. The second dataset is from "THU-FVFDT1" [27] comprising images from 220 individuals. Each individual has two images, with a resolution of 720x576 pixels for the raw images.

Table 1. Details of dataset

Dataset	No. of classes or Individual	No. of fingers per individual	No. of images per finger	Total images
SDUMLA- HMT	106	6	6	3816
THU FV	220	1	2	440

3.2 Finger Vein Image Labelling

Labelling finger vein images involves identifying and marking distinct patterns within the images that correspond to the vein structure. Each pixel in the image is labelled as either vein or background. This allows the deep learning (DL) model to learn the intricate characteristics of the finger vein patterns and enhances the model's sensitivity to subtle changes in vein patterns, which is crucial in applications where high accuracy is required, such as biometric authentication. Pixel-wise labelling ensures that the model learns features specifically related to the vein and background regions, making it more robust to variations in lighting, pose, and other environmental factors. It also facilitates the application of data augmentation techniques at the pixel level; augmenting labelled images by introducing variations in pixel values (e.g., brightness, contrast, or rotation) which helps the model to predict images with variations in enrolled images. Labelled images help reduce ambiguity during training, leading to faster convergence and improved model performance.

We have used automated labelling, which assigns labels or annotations to data automatically without manual intervention. This approach reduces the time and effort required for manual labelling, which is crucial when dealing with vast amounts of data. It is also cost-effective and ensures consistency across the dataset, as the algorithms or rules used to assign labels are applied uniformly.

After extracting the vein region from the original image, a hybrid algorithm that integrates the “Local Maximum Curvature” algorithm, the “Wide Line Detector” algorithm, and the “Repeated Line Tracking” algorithm is used to label the images in the pixel level [6].

The resultant images contain more features compared to those produced by each individual algorithm alone. Sample ROI image and the final labelled image are displayed in Fig. 2.

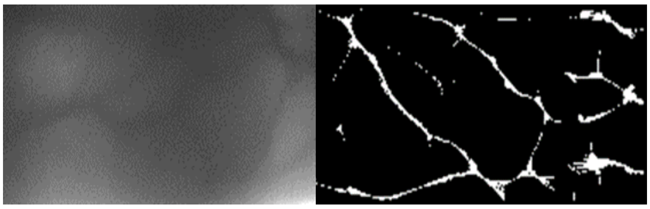

(a) (b)

Fig 2. (i) ROI extracted FV image (ii) Labelled FV image

3.3 Finger Vein Dataset Augmentation

Most finger vein image databases consist of images from different subjects with few images per person. The number of images used for training per person significantly impacts the verification performance of the model. To capture the variability in vein patterns among individuals, a larger dataset is required. A diverse dataset can improve generalization by making the model more robust to different conditions such as rotation, displacement, and lighting variations.

The dataset has been augmented using two strategies. First, using conventional transformations like rotation, shifting, brightness variations, and zooming. Secondly using Generative Adversarial Networks (GAN). Conventional transformations rely on predefined rules and geometric operations, while GANs are deep learning-based methods that require more computational power and complex implementation but can create highly realistic and diverse images. Combining both methods can enhance the dataset for the effective training of deep learning models. Among the transformation methods, systematic rotation helped in creating images at various angles and aids in recognizing images at different angles due to slight variations in finger positioning.

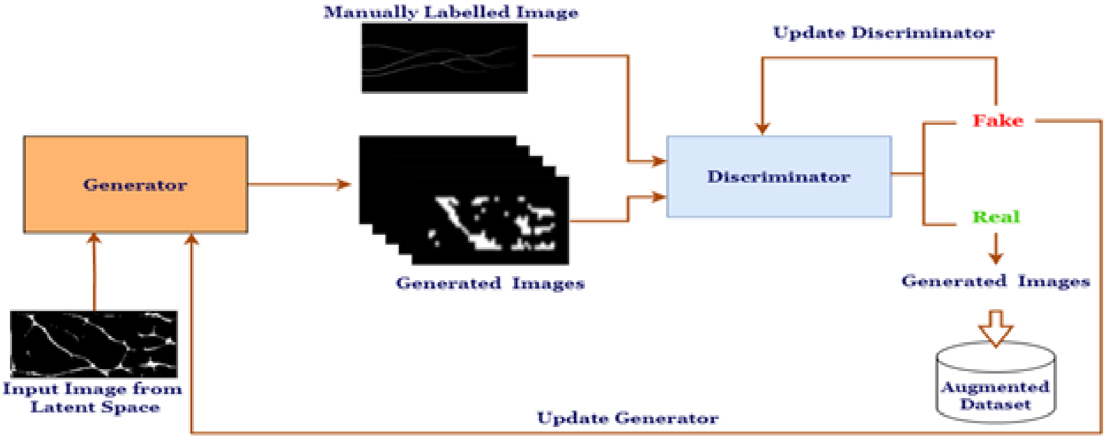

Fig 3. Architecture of cGAN for finger vein dataset

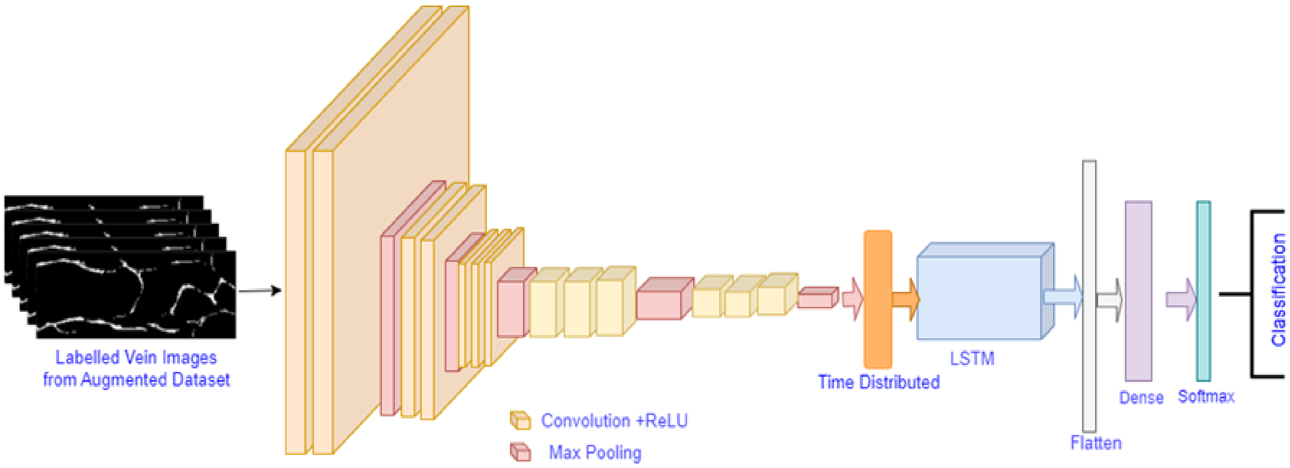

Fig 4. Architecture of motion tolerant deep learning model for finger vein authentication

Shifting helps in making the system less sensitive to small positional shifts of the finger within the capture device. Brightness variations reflect adaptability to different lightning conditions. Zooming helps when the finger may appear at varying distances from the camera. For augmenting using GANs, we employed conditional GANs (cGANs) [28-30]. In cGANs, additional information is provided to the generator and discriminator during training. Manually labelled vein images are given as additional information to the discriminator, helping to maintain the semantic meaning. This approach creates new samples based on the learned features of the dataset, capturing more intricate and complex features of the data distribution, resulting in more realistic and diverse augmented samples. Figure 3 illustrates the architecture of cGAN implemented for finger vein dataset augmentation. The labelled image is inputted as latent vector to the generator. The generator then generates fake images initially and gradually real images after upon training with the feedback from discriminator. The discriminator is also provided with manually labelled images as additional information. If the discriminator output is 'fake image', the feedback is fed to generator and discriminator for training, otherwise the image is added to the dataset.

Algorithm1: Finger Vein Image Dataset Augmentation

Start Algorithm

1. Load Original Dataset:

1.1 Load the original dataset

2. Apply Conventional Augmentation:

2.1 For each image I in the dataset:

2.1.1 Apply rotation transformations to generate images at various angles: I_rot = rotate (I, θ) for θ in A

A: Set of angles used for rotating the images

2.1.2 Apply shifting transformations to generate images with positional shifts:

I_shift = shift (I, δx, δy) for (δx, δy) in S

S: Set of shift values for x and y directions.

2.1.3 Apply brightness variations to simulate different lighting conditions:

I_bright = adjust_brightness (I, β) for β in B

B: Set of brightness adjustment factors

2.1.4 Apply zooming transformations to simulate varying distances:

I_zoom = zoom (I, z) for z in Z

Z: Set of zoom factors.

Combine the augmented images to form D_conv

3. Apply Augmentation using cGANs:

3.1 Initialize cGAN model components:Generator G, Discriminator D

3.2 For each image I labelled as L in the dataset:

3.2.1 Input labelled image L as latent vector to generator G

3.2.2 Generator G generates initial fake image I_fake

3.2.3 Provide labelled image L to discriminator D

3.2.4 Discriminator D evaluates generated image:

output = **D** (I_fake, L)

3.2.5 If output is 'fake image':

3.2.5.1 Provide feedback to G and D for further training

3.2.6 Otherwise if output is 'real image':

3.2.6.1 Add I_fake to D_cGAN

4. Combine Augmented Datasets:

Combine D_conv and D_cGAN to form the final augmented dataset D_aug

End Algorithm

3.4 Proposed Deep Learning Model

The proposed model uses finger vein image sequences for classification. The dataset is pre-processed with image labelling and augmentation techniques. Each sequence groups finger vein images of a single individual. The features are extracted using a VGG16 model, retaining only the convolutional layers of the model. As the fully connected layers are removed, the model becomes lighter and more computationally efficient and focuses solely on feature extraction, without being constrained by the specific task of classification. These layers generate fixed-size feature vectors for each input image. A Time Distributed layer with flattening incorporates temporal information. It processes each image in the sequence independently, reshaping the data for a successive LSTM layer. LSTM layer, with 32 hidden units, learns the relationships between these feature vectors across the sequence. Finally, the sequence is classified by a dense layer with neurons matching the count of classes and a softmax activation function. Fig. 4 shows the architecture of the motion tolerant model.

Algorithm 2: Proposed Deep Learning model

Start Algorithm

1. Data Pre-processing:

1.1. Group the labelled and augmented images into sequences Sj for each individual j: Sj= {Ij,1, Ij, 2…,Ij,T} ,
T : count of images in the sequence
Ij,t : t^{th} image in the sequence of the jth individual

2. Feature Extraction using pre-trained VGG16:

2.1. Initialize the pre-trained VGG16 model.
2.2. Remove the fully connected layers from the VGG16 model.
2.3. For each image Ij,t in sequence Sj:
Fj,t=VGG16_Conv(Ij,t)

3. Incorporate Temporal Information:

3.1. Apply a Time Distributed layer with flattening to each feature vector
Fj,t′=Flatten(Fj,t)

4. Learn Temporal Relationships using LSTM:

4.1. Initialize an LSTM layer with U=32 hidden units.
4.2. For each sequence Sj with flattened feature vectors {Fj,1', Fj,2′…,Fj,T:
Hj=LSTM ([Fj,1′, Fj,2′…,Fj,T′])

5. Classification:

5.1. Initialize a dense layer with c neurons and a SoftMax activation function. (c:number of classes)
5.2. For each hidden state sequence Hj, classify the sequence:
yj=Softmax (WHj+b)

6. Model Training and Evaluation:

6.1. Compile the model with the loss function categorical cross-entropy and Adam Optimizer.
6.2. Train the model on the pre-processed and augmented dataset:
model.fit(sequences, labels, validation_split =0.2, epochs = num_epochs)
6.3. Evaluate the performance on a validation set: model.evaluate (validationset)

End Algorithm

4. Results and Discussion

Different approaches are adopted to assess the model performance on the SDUMLA and THUFV databases. The first approach utilized the VGG16 model with the original dataset. The second approach involved the VGG16 trained on a labelled dataset. The third approach uses the labelled and augmented dataset, to improve model robustness and accuracy. Lastly, the proposed model was evaluated using the labelled and augmented dataset to compare its performance against the VGG16 configurations. These approaches assess the impact of labelling, data augmentation, and model architecture on training time and accuracy.

Table 2 compares performance metrics across different configurations of models trained on two datasets, SDUMLA and THUFV. The results highlight that while augmentation increases training time, the proposed model effectively utilizes labelled and augmented datasets to achieve significantly higher accuracy with reduced training times compared to VGG16, showcasing its robustness and efficiency in finger vein authentication applications.

Table 2. Comparison of performance for various approaches

Data base	Comparison Factor	VGG16 + Original Dataset	VGG16 + Labelled Dataset	VGG16 + Labelled and Augmen-ted Dataset	Proposed Model + Labelled and Augment-ed Dataset
SDUMLA	Training Time (min)	54	36	110	72
	No. of images	424	424	16960	16960
	Accuracy	94.30%	95.45%	97.11%	99.76%
THUFV	Training Time (min)	35	25	85	56
	No. of images	220	220	8800	8800
	Accuracy	92.50%	96.34%	98.60%	99.89%

Comparison of accuracy for various approaches is shown in Table 3. For the “SDUMLA” dataset the accuracy of VGG16 on the initial dataset was 94.30%, which improved to 95.45% with the labelled dataset. With the labelled and augmented dataset, the accuracy further increased to 97.11%. The proposed model achieved 99.76% accuracy with the labelled and augmented dataset, indicating superior performance. For the THUFV dataset the accuracy of VGG16 on the original dataset was 92.50%, improving to 96.34% with the labelled dataset. Using the labelled and augmented dataset, the accuracy increased to 98.60%. The proposed motion tolerant model achieved an accuracy of 99.89% on the labelled and augmented dataset, demonstrating the best performance among all configurations.

Table 3. Accuracy obtained on SDUMLA and THUFV Database

Database	VGG16 + Original Dataset	VGG16 + Labelled Dataset	VGG16 + Labelled and Augment ed Dataset	Proposed Model + Labelled and Augmented Dataset
SDUMLA	94.3%	95.45%	97.11%	**99.76%**
THUFV	92.5%	96.34%	98.6%	**99.89%**

Figure 5 shows the accuracy graphs for the proposed model trained on the THUFV dataset over 40 epochs and the SDUMLA dataset over 25 epochs. For the THUFV dataset, the model's accuracy began to stabilize around the 20th epoch, showing a clear trend towards convergence. By the end of training, the model achieved a remarkable accuracy of 99.89%. Similarly, on the SDUMLA dataset, the model's convergence was observed slightly earlier, starting to stabilize around the 10th epoch. Despite a shorter training duration of 25 epochs, the model attained a high accuracy of 99.76%. This underscores the robustness of the proposed motion tolerant model architecture and its capability to handle variations in finger vein patterns across different datasets. This indicates that the model effectively learned the intricate patterns within the finger vein images from both the dataset, showing its ability to generalize and make accurate predictions.

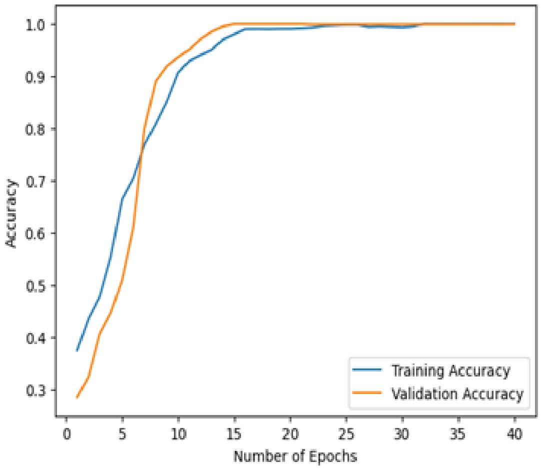

(a)

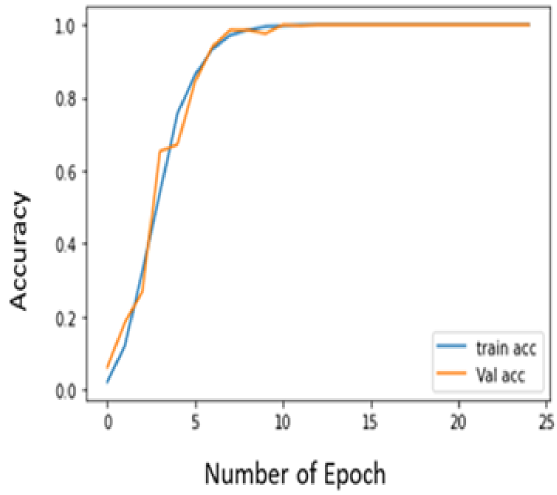

(b)

Fig. 5. The accuracy graph for the proposed motion tolerant model using labelled and augmented dataset (a) THUFV Dataset (b) SDUMLA Dataset

Figure 6 shows the plot of Receiver Operating Characteristic (ROC) plotted at varying threshold settings to evaluate the model's performance. “Equal Error Rate (EER)” represents the point where false rejection and acceptance rates are equal, indicating when positives and negatives are equally likely. “Area Under the Curve (AUC)” is a measure of how well the model differentiates between positive and negative classes. The ROC for the proposed model using labelled and augmented dataset is depicted in Fig. 6. The EER for SDUMLA and THUFV dataset are 1.73% and 1.42% respectively. The area under the curve for SDUMLA and THUFV are 0.993 and 0.991 respectively, which are close to 1. Both the EER and AUC metrics indicate a highly effective classification system for both databases.

Table 5. EER and AUC vales for SDUMLA and THUFV Database

Database	*EER*	*AUC*
SDUMLA	1.73%	0.993
THUFV	1.42%	0.991

The proposed model also demonstrates better efficiency in training time compared to VGG16 under similar conditions which is detailed in table 4. For the SDUMLA database, training the VGG16 model on the original dataset took 54 minutes, while using the labelled dataset reduced this time to 36 minutes. Training on the labelled and augmented dataset increased the time to 110 minutes. The proposed model with the labelled and augmented dataset required 72 minutes. Similarly, for training original THUFV database on VGG16 took 35 minutes, and on the labelled dataset, it reduced to 25 minutes. Training on the labelled and augmented dataset took 85 minutes, while the proposed model with the labelled and augmented dataset needed 56 minutes. Overall, while augmentation increases training time, the proposed model offers a balance with improved performance over the VGG16 with labelled and augmented datasets.

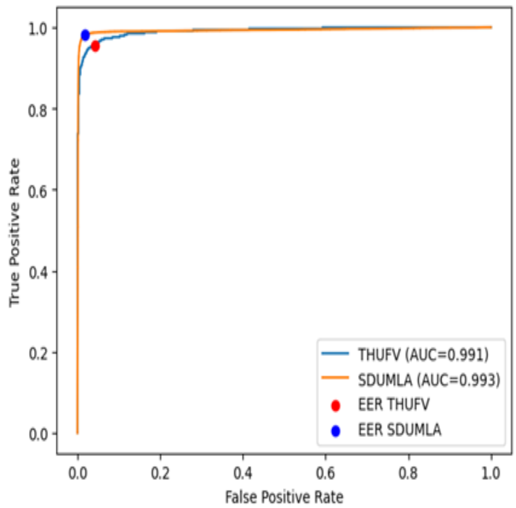

Fig 6. ROC for the proposed motion tolerant model using labelled and augmented dataset for SDUMLA Dataset and THUFV Dataset

Table 4. Training time (in minutes) on SDUMLA and THUFV Database

Database	**VGG16 + Original Dataset**	**VGG16 + Labelled Dataset**	**VGG16 + Labelled and Augmented Dataset**	**Proposed Model + Labelled and Augmented Dataset**
SDUMLA	54	36	110	72
THUFV	35	25	85	56

5. Conclusion

The study demonstrates that finger vein authentication systems can significantly benefit from image labelling, data augmentation, and advanced model architectures to improve performance and robustness. Evaluations on the SDUMLA and THUFV databases reveal that while the VGG16 model performs well on original datasets, its accuracy substantially improves with labelled datasets and further with labelled and augmented datasets. The proposed model, incorporating a combination of VGG16 and LSTM networks, achieves the highest accuracy and demonstrates superior performance over VGG16 configurations, achieving 99.76% accuracy on SDUMLA dataset and 99.89% accuracy on THUFV dataset. Moreover, the proposed model exhibits better training efficiency, balancing increased training time due to augmentation with enhanced accuracy and robustness. The ROC and AUC metrics confirm the high effectiveness of the proposed system, underscoring its potential for reliable biometric authentication in real-world applications.

Overall, the integration of labelling, augmentation, and a motion-tolerant deep learning architecture represents a significant step in the development of secure and accurate finger vein authentication systems.

Author contributions

Amitha Mathew (Corresponding author): Developing an original draft, studying methodology, conceiving and designing the study, reviewing and editing it, analysis and interpretation of results

***Dr.* P. Amudha:** Concept development, Reviewing and editing.

Conflicts of interest

The authors declare no conflicts of interest.

References

[1] Liu, C. Y., Ruan, S. J., Lai, Y. R., & Yao, C. Y. (2019). Finger-vein as a biometric-based authentication. IEEE Consumer Electronics Magazine, 8(6), 29-34.

[2] Shaheed, K., Mao, A., Qureshi, I., Kumar, M., Hussain, S., & Zhang, X. (2022). Recent advancements in finger vein recognition technology: methodology, challenges and opportunities. Information Fusion, 79, 84-109.

[3] Wang, K., Ma, H., Popoola, O. P., & Li, J. (2011). Finger vein recognition. Biometrics, 31-53.

[4] Simonyan K, Zisserman A. Very deep convolutional networks for large-scale image recognition. arXiv preprint arXiv:1409.1556. 5 Sep 2014.

[5] Hochreiter, S., & Schmidhuber, J. Long short-term memory. Neural computation, 9(8), 1735-1780, 1997.

[6] Zhang, K., Chao, W. L., Sha, F., & Grauman, K. Video summarization with long short-term memory. In Computer Vision–ECCV 2016: 14th European Conference, Amsterdam, The Netherlands, October 11–14, 2016, Proceedings, Part VII 14 (pp. 766-782). Springer International Publishing.

[7] Qin, H., & Wang, P. Finger-vein verification based on LSTM recurrent neural networks. Applied Sciences, 9(8), 1687, 2019

[8] Kauba, C., & Uhl, A. An available open-source vein recognition framework. Handbook of Vascular Biometrics, 113-142, 2020

[9] A. Mathew, P. Amudha, and S. Sivakumari, "Finger Vein Image Labelling using Hybrid Algorithm," International Conference on Emerging Trends in Industry 4.0 and Sustainable Concepts, 2023, pp. 268-271

[10] Scantlebury, J., Brown, N., Von Delft, F., & Deane, C. M. Data set augmentation allows deep learning-based virtual screening to better generalize to unseen target classes and highlight important binding interactions. Journal of chemical information and modeling, 60(8), 3722-3730,2020

[11] Shorten, C., & Khoshgoftaar, T. M. A survey on image data augmentation for deep learning. Journal of big data, 6(1), 1-48, 2019

[12] Mikołajczyk, A., & Grochowski, M. Data augmentation for improving deep learning in image classification problem. In 2018 international interdisciplinary PhD workshop (IIPhDW) (pp. 117-122). IEEE, May 2018

[13] Taylor, L., & Nitschke, G. Improving deep learning with generic data augmentation. In 2018 IEEE symposium series on computational intelligence (SSCI) (pp. 1542-1547). IEEE, November 2018.

[14] Perez, L., & Wang, J. The effectiveness of data augmentation in image classification using deep learning, 2017. arXiv preprint arXiv:1712.04621.

[15] Kuzu, R. S., Piciucco, E., Maiorana, E., & Campisi, P. On-the-fly finger-vein-based biometric recognition using deep neural networks. IEEE Transactions on information Forensics and Security, 15, 2641-2654, 2020.

[16] Y. Yamagishi and S. Maeda, "Deep Learning of Convolutional Neural Networks for Finger Vein Authentication," IET Biometrics, vol. 6, no. 3, pp. 217-226, 2017.

[17] S. A. Radzi, M. Khalil-Hani, and R. Bakhteri, "Finger-vein biometric identification using convolutional neural network," Turkish Journal of Electrical Engineering & Computer Sciences, vol. 24, no. 3, pp. 1863-1878, 2016.

[18] H. Qin and M. A. El-Yacoubi, "Deep representation-based feature extraction and recovering for finger-vein verification," IEEE Transactions on Information Forensics and Security, vol. 12, no. 8, pp. 1816-1829, Aug. 2017.

[19] H. G. Hong, M. B. Lee, and K. R. Park, "Convolutional Neural Network-Based Finger-Vein Recognition Using NIR Image Sensors," Sensors, vol. 17, no. 6, pp. 1297, 2017.

[20] E. Jalilian and A. Uhl, "Finger-vein recognition using deep fully convolutional neural semantic segmentation networks: The impact of training data," in IEEE International Workshop on Information Forensics and Security (WIFS), Hong Kong, China, 2018, pp. 1-7.

[21] Y. Fang, Q. Wu, and W. Kang, "A novel finger vein verification system based on two-stream convolutional network learning," Neurocomputing, vol. 290, pp. 132-143, May 2018.

[22] W. Kim, J. M. Song, and K. R. Park, "Multimodal biometric recognition based on convolutional neural network by the fusion of finger-vein and finger shape using near-infrared (NIR) camera sensor," Sensors, vol. 18, no. 1, pp. 101-114, Jan. 2018.

[23] M. Frid-Adar, I. Diamant, E. Klang, M. Amitai, J. Goldberger, and H. Greenspan, "GAN-based synthetic medical image augmentation for increased CNN performance in liver lesion classification," Neurocomputing, vol. 321, pp. 321-331, 2018.

[24] C. Bowles, L. Chen, R. Guerrero, P. Bentley, B. Glocker, and D. Rueckert, "GAN augmentation: Augmenting training data using generative adversarial networks," arXiv preprint arXiv:1810.10863, 2018.

[25] R. S. Kuzu, E. Piciucco, E. Maiorana, and P. Campisi, "On-the-fly finger-vein-based biometric recognition using deep neural networks," IEEE Transactions on Information Forensics and Security, vol. 15, pp. 3104-3118, 2020.

[26] Yin, Y., Liu, L., Sun, X. (2011). SDUMLA-HMT: A Multimodal Biometric Database. In: Sun, Z., Lai, J., Chen, X., Tan, T. (eds) Biometric Recognition. CCBR 2011. Lecture Notes in Computer Science, vol 7098. Springer, Berlin, Heidelberg.

[27] Tsinghua University Finger Vein and Finger Dorsal Texture Database（THU-FVFDT）. (2014). [Dataset]. In Wenming Yang.

[28] Mirza M, Osindero S. Conditional generative adversarial nets. arXiv preprint arXiv:1411.1784. Nov 6, 2014.

[29] Xie C, Kumar A. Finger vein identification using convolutional neural network and supervised discrete hashing. Deep Learning for Biometrics. 2017, pp.109-32.

[30] Bilal, A., Sun, G. and Mazhar, S., Finger-vein recognition using a novel enhancement method with convolutional neural network. Journal of the Chinese Institute of Engineers, 44(5), 2021, pp.407-417.